Chemical Engineering Journal 482 (2024) 148861

Contents lists available at ScienceDirect

Chemical Engineering Journal

journal homepage: www.elsevier.com/locate/cej

Towards a better understanding of the cosolvent effect on the low-temperature glycolysis of Polyethylene Terephthalate (PET)

Emelin Luna [a,b], Ion Olazabal [a], Martijn Roosen [b], Alejandro Müller [a], Coralie Jehanno [c], Marta Ximenis [a], Steven de Meester [b,*], Haritz Sardon [a,*]

[a] POLYMAT, University of the Basque Country UPV/EHU, Avda. Tolosa 72, 20018, Donostia-San Sebastian, Spain
[b] Department of Green Chemistry and Technology, Ghent University, Graaf Karel De Goedelaan 5, Kortrijk 8500, Belgium
[c] POLYKEY, Avda. Tolosa 72, 20018, Donostia-San Sebastian, Spain

ARTICLE INFO

Keywords:
Polyethylene Terephthalate (PET)
Cosolvent
Glycolysis
Solvolysis
LCA
Chemical recycling

ABSTRACT

As the demand of polyethylene terephthalate (PET) increases worldwide along with the waste generated from its use, it is urgent to develop cost-efficient and sustainable recycling processes, such as depolymerization that yields monomers with virgin-like qualities. However, most of these processes require harsh conditions and their true mechanisms are poorly understood, leading to marginal gains in energy efficiency and yield. In spite of the lack of solubility of PET, we demonstrate that the swelling and plastification of PET in a good solvent allows a better mass transport of ethylene glycol and the catalyst into the polymer during glycolysis. Based on these insights, we report a process in which PET is depolymerized into bis(2-hydroxyethyl)terephthalate (BHET) with a yield of 88 % at 65 °C within 1 h in the presence of 1,3-Dioxolane as green cosolvent carrier. The improved mass transport allows to perform the depolymerization of PET even below the T_g of the polymer. Indeed, by kinetic modelling we demonstrated that a heterogeneous depolymerization process could be easily transformed into an homogeneous process by an appropriate solvent selection. The environmental impact of the proposed process, including solvent recovery, is compared to the solvent-free counterpart and the results demonstrates that by using 1,3-Dioxolane, the carbon footprint of the newly developed glycolysis process can be reduced up to 20 % due to the increased energy efficiency. This process enables a viable recycling strategy of PET into its repetitive unit, contributing to the development of competitive chemical recycling solutions to reduce PET-derived pollution.

1. Introduction

Poly(ethylene terephthalate) (PET) is the most used condensation polymer worldwide [1]. The combined mechanical and chemical properties of this material allow its application in the production of bottles, trays and flexible packaging, as well as in the textiles industry. According to Plastics Europe (2022), the world PET production amounted to 24.2 million tonnes (Mt) in 2021. From this, merely 21 % was recycled in 2020 and used in food and non-food packaging as well as in the fabrication of monofilament and fiber products [2]. The largest part of the recycled PET fraction consists of clear and light blue bottles, primarily due to the lack of widespread recycling approaches for the more complex PET waste streams [3]. The presence of pigments and dyes and other impurities at variable concentrations affects negatively the quality of the material recovered by mechanical recycling. An alternative to mechanical recycling is solvolysis, a chemical recycling process in which the discarded polyester is transformed into its precursors or into new chemicals with a virgin-like quality by a transesterification reaction [4]. Depending on the nature of the solvent used as nucleophile, solvolysis of PET is typically classified into five methods: hydrolysis [5], methanolysis [6], glycolysis [7], aminolysis [8], and ammonolysis [9].

Glycolysis is by far the most explored process due to its simplicity and lowest capital requirements [10]. In principle, the reactive solvent is ethylene glycol (EG), combined with organometallics catalysts or alternatively strong, bifunctional bases like triazabicyclodecene (TBD) or its ionic salts with methanesulfonic acid (TBD:MSA) as well as TBD-based oxoacid protic ionic salts [11–13]. In the first stages of the reaction, the polymeric chains in the proximities of the surface of the solid PET sample are broken into oligomers, then dimers, and finally into bis (2-hydroxyethyl)terephthalate (BHET), the precursor of the material [14]. The diffusion of the liquid phase, comprising the ethylene glycol (EG) and the dissolved catalyst into the polymer matrix is extremely

* Corresponding authors.
E-mail addresses: Steven.DeMeester@UGent.be (S. de Meester), haritz.sardon@ehu.es (H. Sardon).

https://doi.org/10.1016/j.cej.2024.148861

Available online 18 January 2024
1385-8947/© 2024 The Authors. Published by Elsevier B.V. This is an open access article under the CC BY-NC license (http://creativecommons.org/licenses/by-nc/4.0/).

Table 1
Exemplary reaction conditions of different glycolysis processes reported in literature.

EG:PET	Yield (%)	T (°C)	Time (min)	Catalyst	Ref.
12.6	88	190	100	Si-TBD	[17]
15	91	180	120	TBD:MSA	[11]
16	78	190	210	TBD	[12]
7.6	80	196	60	Na_2CO_3	[18]
13	86	180	90	Zinc Acetate	[19]

important as the reaction is not possible if the molecules in the fluid are not able to reach the C-O bond of the ester. The latter was demonstrated by Pardal and Tersac during their studies regarding the reactivity of different glycols in the PET depolymerization and the reaction kinetics at 220 °C when an excess of EG was used as reactive solvent [15,16]. By following the changes in both the liquid and solid phases, they observed that the reaction started with the swelling of the polymer due to the diffusion of the glycol into the amorphous interlamellar segments, increasing the diffusion rate. In parallel, they also found that during the reaction the formed oligomers and the BHET diffused to the liquid phase, until the solid disappeared completely.

However, EG is characterized by its poor solvation ability of the polymer at low temperatures [15]. In fact, PET is insoluble in most solvents. Therefore, it is not surprising that in most processes reported in literature, the glycolysis reaction temperature is above 190 °C, a value close to the EG boiling point (197 °C at 1 bar; see Table 1). The high reaction temperature and long batch times make the process energetic intensive. Moreover, if the produced BHET is recovered either by co-precipitation using an antisolvent or by evaporation of the EG, the energy demands of the process increases as consequence of the low vapour pressure of the glycol, increasing the product purification costs [4].

Therefore, it is imperative to conduct research with the aim to perform PET glycolysis in a manner that is more energy and cost-efficient [4]. The use of cosolvents as a strategy to reduce the reaction temperature and time has been proposed by several authors. For instance, Liu et al. explored the effect of solvents capable to dissolve the polyester, such as DMSO, using zinc acetate ($Zn(OAc)_2$) as catalyst at 170 °C, reaching a total conversion of PET after 5 min and BHET yields of 82 % [20]. Furthermore, Le et al. carried out the reaction at 150 °C using anisole as green co-solvent and KOAc as catalyst, reaching a total PET decomposition into BHET and short-chain oligomers after 2 h [21].

However, the reaction conditions reported in these works remain comparable to those previously documented in the literature. Additionally, a detailed explanation of the effect of the cosolvent on the reaction is not yet well established. In addition, the previous studies considered only the potential improvement in terms of the energy consumption in the reaction stage, leaving aside the global impact of cosolvent addition on the process, which is very relevant in the purification stage of the monomer [22].

In 2017, Loop Industries demonstrated that the methanolysis of PET could be performed at room temperature in 24 h by adding dichloromethane (DCM) as cosolvents and KOH as catalyst [23]. DCM is a solvent that has been previously reported for its capability to swell polyester at temperatures below its boiling point (39.6 °C at 1 bar) [24]. Recently, this phenomenon was also illustrated by Zhang et al., notably in their work on the hydrolysis of PET, in which they reported the conversion of the polyester into terephthalic acid (TPA) at 35 °C in 15 min using a blend of DCM/Ethanol as liquid phase and KOH as catalyst [25]. However, as DCM is a halogenated solvent, its usage in systems that aim for a more sustainable economy for polymer waste is not desired. Additionally, its nature may cause an increase of costs related with process safety management derived from its low boiling point [26]. Besides, Huang et al. claimed that when using acetonitrile as cosolvent in presence of a choline chloride (ChCl)/$Zn(OAc)_2$ deep-eutectic solvent (DES) catalyst, glycolysis was possible at 90 °C in 12 h. The authors

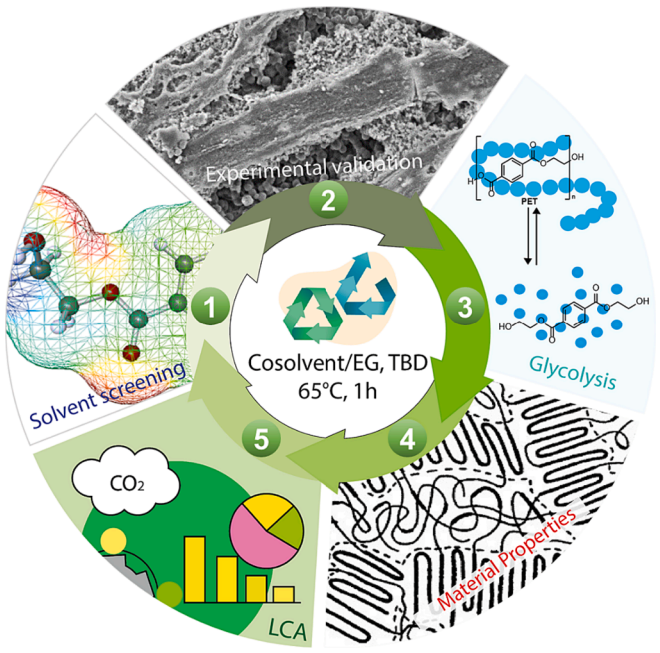

Fig. 1. Schematic overview of the methodology followed to study the impact of cosolvents on PET depolymerization. In the first two stages the solvent selection and the experimental validation of the interaction among solvents and the material is carried out. In the third stage, we did the reaction in the different solvents. Moreover, the reaction kinetics was followed. In the fourth stage, the effect of PET crystallinity on the BHET yield using the reaction conditions considered as optimal is evaluated. Finally, a Life Cycle Assessment (LCA) comparing the effect current process with the incineration benchmark scenario and the solvent-free scenario.

concluded that the swelling induced by acetonitrile on PET chips could help to accelerate the reaction at low temperature, although the effect of the solvent on the material was not studied deeply [27].

To allow a better design of such a solvent assisted depolymerization, it seems that a deep understanding of the mechanism involved is lacking, which hampers solvent/catalyst/condition choices. In this paper, we aim to deliver such understanding by first screening a set of solvents that are chemically inert to the basic environment needed for solvolysis by studying the solvents' selectivity for PET utilizing theoretical tools such as the Hansen solubility parameters (HSP) and Conductor-Like screening model for realistic solvation (COSMO-RS).

Then, we experimentally validate the insights obtained from the theoretical study by means of solvent uptake studies, differential scanning calorimetry (DSC), and scanning electron microscopy (SEM) using model PET samples. The effectiveness of the solvents selected was tested in the PET glycolysis at the established reaction conditions, demonstrating that when cyclic ethers and acetals are added in the liquid phase as cosolvents along with EG, the glycolysis reaction is possible below the glass transition temperature of the material in 1 h. Moreover, we measured the optimal cosolvent:PET molar ratio required to reach the highest possible monomer yield while minimizing the yield of lower oligomers.

Next, the effect of the cosolvent in the reaction was studied by determining the best-fitting kinetic model from the experimental kinetic data in different cosolvents. Furthermore, we carried out depolymerization trials in high crystalline model samples to elucidate the cosolvent role as carrier of the EG and the catalyst within the free volume available in the polymer. As expected, the higher the crystallinity of the sample, the lower is the conversion of PET into monomer and oligomers. Finally, we studied the energy balance and the environmental performance of the cosolvent assisted glycolysis scenario compared to the cosolvent-free EG based glycolysis scenario by performing carbon footprint

calculations, finding that with our approach up to 20 % of CO_2 can be saved.

The overall methodology applied in this study is graphically shown in Fig. 1.

2. Materials and methods

2.1. Chemicals and materials

For the polymer–solvent interaction experiments, PET pellets from Novapet CR® were used. Postconsumer transparent PET water bottles were cut manually into flakes of 1 cm x 0.5 cm and washed two times with methanol after removing caps, labels, and glue. Subsequently, the flakes were dried in an oven at 60 °C for 24 h. The number average molecular weight (Mn) was calculated through ^{1}H NMR spectroscopy following the procedure proposed by several authors previously [28–32]. The polymer was dissolved in a mixture of deuterated chloroform ($CDCl_3$) and trifluoroacetic acid (TFA) (8:1, v/v) and then the measurements were carried out in a Bruker Advance 400 (400 MHz) spectrometer. The same approach was applied to calculate the Mn of virgin PET pellets. All the spectra were referenced to $CDCl_3$. All solvents and other chemicals were obtained from Sigma-Aldrich and used without further purification (purities $\geq$ 98 %).

2.2. Solvent selection theoretical tools

2.2.1. Hansen solubility parameters (HSPs)

HSPs are important physicochemical parameters to predict solubility relations between polymers and solvents [33]. The basis of these parameters is that the total energy of vaporization is equivalent to the total cohesion energy, whereby the former represents the sum of the individual energies or interactions that make it up [34]. These interactions are represented by the three solubility parameters: dispersion (δ_d), polar (δ_p), and hydrogen bonding (δ_h). The Equation (1) calculated the solubility parameter Ra, which represents the distance between the HSP of two materials:

$$(R_a)^2 = 4\left(\delta_{d,A} - \delta_{d,S}\right)^2 + \left(\delta_{p,A} - \delta_{p,S}\right)^2 + \left(\delta_{h,A} - \delta_{h,S}\right)^2 \quad (1)$$

Therefore, the smaller the Ra value, the stronger the affinity is between the solvent and the polymer.

2.2.2. Conductor-Like screening model for realistic solvation (COSMO-RS)

COSMO-RS offers an efficient and general route to determine thermodynamic properties such as the activity coefficients and excess enthalpies of systems composed by unlike species (e.g., PET-Solvents). The basic idea is to compute the chemical potential in solution or, in this case, in a polymer via fast statistical thermodynamics of interacting molecular surface segments which are derived from quantum chemical calculations in a continuum solvation model [35]. The COSMO-RS calculations were carried through a sequence of several simulation steps. First, the geometries of PET and the solvents evaluated were drawn in GaussView 6.0.16. The Gaussian 16 package was used to optimize the geometries of the analysed molecules at B3LYP (Becke 3-parameter hybrid functional combined with the Lee– Yang–Parr correlation) theory and 6–311 + G(d, p) basis set. Frequency calculations were also performed to verify the optimized structures and energy minima. The creation of the Cosmo file was carried out following the methodology described elsewhere and processed with Biovia Cosmotherm 20.0.0 (Dassault Systèmes) [2-4].

To get a better understanding of the phenomenon occurring among the solvents selected in the first screening with PET, the activity coefficients (γ) for each PET-Solvent system were calculated at 65 °C, as shown in Equation (2):

$$\gamma_I = exp\left(\frac{\mu_i - \mu_i^0}{RT}\right) \quad (2)$$

This parameter is critical to determine the ability of a solvent to interact with a solute. The temperature value was selected in base of previous studies made regarding the interaction among PET with different organic solvents as well as the outcomes obtained from the HSP based pre-screening step regarding Ra value of the solvents evaluated, being Tetrahydrofuran (THF) (66 °C at 1 bar) one of the species with the lowest Ra and boiling point [36,37]. For the solvents selected in the pre-screening stage, we used pre-calculated COSMO files from the database COSMObase-1901-BP-TZVP.

2.3. Determining solvents' effect on PET

2.3.1. Preparation of model samples

Model PET samples with a 1.8 mm thickness were taken from virgin PET plates made by hot pressing 5 g of pellets in a Collin P200C hydraulic press. The moulding process lasted 10 min at 295 °C in both moulds with a plasticization time of 7 min, followed by the application of a 200 bar load for a period of 2 min, which was sustained for an additional 1 min. For amorphous samples, the melt was removed from the press immediately after completing the compression time and submerged in water at 4 °C for 30 s. Then, the transparent plates were put to dry in a vacuum oven for 24 h at 80 °C. After this, the sample was kept at room temperature in a desiccator for another 24 h. Finally, the model samples of 1 cm x 0.5 cm were cut from the plates with a cutter. The crystallinity of the model samples was calculated by the Equation (3):

$$X_c = \frac{\Delta H_m - \Delta H_{CC}}{\Delta H_{m(100\%)}} \quad (3)$$

where X_c is the crystalline mass fraction. A $\Delta H_{m(100\%)}$ of 140 J/g was used for all the calculations. The thermal characterization of the samples was carried out in a TA Instruments DSC 25 under 50 mL/min of nitrogen flow.

2.3.2. Swelling studies

Swelling experiments were carried out on the model PET particles adapting the methodology described by Haga [24]. Model samples of 0.2 $\pm$ 0.01 g were put in the liquid solvent for 1 h at 65 °C. During this period, the temperature of the solvent was monitored using a Hanna Checktemp HI98509 Digital Thermometer. Then, the PET particles were removed from the solvent and the excess liquid was dried from the particle surface using filter paper. The solvent uptake was calculated by the following Equation (4):

$$Solventuptake = \frac{\rho_1(w_2 - w_1)}{\rho_2 w_1} \times 100 \quad (4)$$

where w_1 and w_2 represent the weights of PET before and after the swelling, and ρ_1 and ρ_2 the densities of PET and the solvent, respectively. The density of the PET samples was of 1.34 g/cm^3 and the value was measured by volume displacement of distillate water in a graduated cylinder at 25 °C. Each experimental point was repeated three times.

2.3.3. Scanning electron microscopy (SEM)

The surface morphologies of some of the specimens treated during the swelling essays were observed by SEM. The samples were washed out with distilled boiling water for 1 h in order to remove the solvents trapped inside the particle as these must be dry before the gold coating. Finally, the water excess was removed with filter paper and the samples were dried in a vacuum oven at 80 °C for 24 h. A Hitachi TM3030Plus electron microscope operated at an accelerating voltage of 15 kV was used to study the specimens [38,39].

2.3.4. Solvent effect over PET T_g

Polymer swelling can lead to the reduction of the glass transition temperature (T_g) by the effect of plasticization [40]. To verify this phenomenon, the same procedure described in the solvent uptake experiment was followed but this time 15 ± 1.0 mg of the sample was put into the aluminium hermetic sealed pan with a pinhole for DSC measurements. A TA Instruments DSC 25 was used for this experiment. An aluminium pan with the same weight was used as the reference. The temperature program involved a heating rate of 30 °C/min until reaching 100 °C, followed by a cooling rate of 10 °C/min until returning to 25 °C, all under nitrogen atmosphere. Additionally, dynamic mechanical analysis (DMTA) measurements were performed in a Triton 2000 DMA (Triton Technology). The measurements were carried out on 6 mm × 5 mm × 1 mm virgin PET samples in a single cantilever bending mode at a single frequency of 1 Hz. The samples were cooled down to −75 °C and heated with a constant temperature ramp of 3 °C/min until 100 °C.

2.4. Solvent-assisted glycolysis experiments

To investigate the effect of the use of co-solvents on the degradation of PET below its T_g, 1 g of PET flakes with a particle size of 5 mm × 5 mm were used in all experimental runs. We selected TBD as organocatalysts due to its proved high activity and selectivity in the depolymerization of polyesters [12,41]. The cosolvents, along with the EG, the catalyst, and N-Dimethylformamide (DMF) as internal standard, were preheated to 40 °C in a two-neck round bottom flask, while the system was mixed by a magnetic stirrer [11]. A stirring rate of 500 rpm was adjusted to have constant mixing during all the tests. Subsequently, the PET flakes were added and the system was heated to the reaction temperature. Each experiment was carried out three times. The quantities of the compounds used in each cosolvent trial is listed in Table S2. For the crude product reaction characterization, an aliquot of 4 μL was withdrawn at certain reaction times to follow the progress of the system until the end of the reaction was reached. As the monomer can aggregate after several hours when the system is at room temperature, purification of the crude was carried out immediately after concluding the reaction time. At this point, the reaction crude was hot filtrated to remove the insoluble oligomers and the unconverted PET flakes from the crude. The flakes were washed two times with methanol, and subsequently dried overnight at 60 °C. Afterwards, hot water was added to the filtrate and a second filtration was carried out to remove the soluble oligomers after stirring at constant temperature, which were dried overnight in a vacuum oven at 80 °C. The second filtrate was partially evaporated until reaching saturation of the solution, and then stored in a refrigerator at 4 °C overnight. Finally, the white needle-like crystals formed were separated from the mother liquor by filtration, and subsequently subjected to a drying process at 80 °C for 24 h. The yield of BHET in the reaction crude was measured by ^{1}H NMR in $CDCl_3$ and calculated by the Equation (5):

$$y_{BHET} = \frac{A_3}{A_{BHET_{x=1}}} - \frac{A_4}{A_{O_{x=1}}} \tag{5}$$

In which A_3 is the integrated area below the BHET signal, $A_{BHETx=1}$ the area below the pure BHET signal (equal to 4), A_4 the area below the oligomer signal, and $A_{Ox=1}$ the area below the pure oligomer signal (equal to 4). All samples were prepared with aliquots of 4 μL dissolved in 0.4 mL of deuterated solvent. ^{1}H NMR, and FTIR spectroscopic characterizations revealed the crystals to be highly pure BHET monomer when compared to commercially supplied BHET. The oligomer yield is determined by Equation (6):

$$PET_{t_0} = PET_{t_f} + BHET + Oligomers \tag{6}$$

Where PET_{t_0} is the normalized molar fraction the PET flakes at time 0, BHET the yield of the monomer in the reaction crude measured by ^{1}H NMR, and PET_{t_f} the molar fraction of unconverted PET flakes recovered during the hot filtration calculated following Equation (7):

$$X_{PET} = \frac{m_{PET,0} - m_{PET,t}}{m_{PET,0}} \tag{7}$$

The reaction and monomer recovery steps are illustrated in Fig. S2.

2.5. Reaction kinetics studies

The glycolysis of PET is a complex reaction in which chemical interactions and mass transfer phenomena are occurring simultaneously [42]. In previous studies regarding the solvolysis of PET, the kinetic models evaluated were classified based on assumptions made regarding the phases involved as homogeneous and heterogeneous [43,44]. For instance, Campanelli et al. [45] proposed a homogeneous 1st order kinetic model for its reaction at 245 °C; conditions at which the treated PET is in molten state. However, the contribution of the reverse reaction was not considered, which is crucial as a monomer-oligomer equilibrium is stablished at the last stages of the reaction [46]. In addition, Fonseca et al. [18] concluded that PET glycolysis took place as a 2nd order homogeneous reaction in which the kinetic rate-determining step was the formation of the monomer from the oligomer in the liquid phase until equilibrium is reached. On the other hand, for the heterogeneous models the reaction evolves from a solid–liquid biphasic system to a single-phase one [19,42,47]. As the system we are proposing for the PET glycolysis takes place far below the melting point of the material, we first assessed a heterogeneous kinetic model, being the shrinkage particle or shrinking core [48]. In addition, the equilibrium limited homogeneous kinetic model as well as a direct reaction model were evaluated.

According to the shrinking particle model, the particle changes its surface along the reaction as the conversion towards the product increases. Therefore, the reaction takes place on the surface of the PET particle and stops when the particle disappears. [48] Then, the decrease of the volume V of a PET spherical particle having a density equal to ρ_{PET} that occurs along the disappearance of the dN_{PET} moles of PET is given by Equation (8):

$$-dN_{PET} = -bdN_{EG} = -\rho_{PET}dV = -4\pi\rho_{PET}r_c^2 dr_c \tag{8}$$

The rate of disappearance of the PET particle is described by Equation (9):

$$-\frac{1}{S_e}\frac{dN_{PET}}{dt} = -\frac{\rho_{PET}r_c^2}{R^2}\frac{dr_c}{dt} = bk_g C_{EG} \tag{9}$$

k_g is the mass transfer coefficient between the bulk solid and liquid and S_e the unchanged surface of the particle. Two special cases of this model are defined. In the first, the process is controlled mainly by the chemical reaction and with little effects from the diffusion resistances. In the second, the diffusion resistance controls the reaction kinetics.

When the chemical reaction controls over the mass transfer and no ash layer is formed around the particle, the rate of reaction is proportional to the surface available of unreacted core and the general expression becomes:

$$-\frac{1}{4\pi r_c^2}\rho_{PET}4\pi r_c^2\frac{dr_c}{dt} = -\rho_{PET}\frac{dr_c}{dt} = bk^{"}C_{EG} \tag{10}$$

$k^{"}$ is the first-order rate constant for the surface reaction, b is the stoichiometric coefficient of EG. By integrating Equation (10), we get the following expression that describes the time required to convert a spherical particle of PET or when $r_c = 0$:

$$K_c t = 1 - (1 - X_{PET})^{1/3} \tag{11}$$

where:

Table 2
Kinetic models evaluated.

Symbol	Reaction model	Linearized form
HE_1	Shrinking particle model (Contracting Volume)	$1-(1-X_{PET})^{1/3}$
HE_2	Shrinking particle model (Diffusion controlled)	$1-(1-X_{PET})^{2/3}$
HO_1	Equilibriun limited, second order homogeneous model	$-ln\left(1-\frac{X_{PET}}{X_e}\right)$
HO_2	Second order homogeneous model	$(1-X_{PET})^{-1}-1$

$$K_c = \frac{bk^{''}C_{EG,s}}{\rho_{PET}R} \tag{12}$$

On the other hand, when the reaction is diffusion controlled, the expression becomes as follows:

$$K_d t = 1-(1-X_{PET})^{2/3} \tag{13}$$

where:

$$K_d = \frac{2bC_{EG,s}\mathscr{D}}{\rho_{PET}R_0^2} \tag{14}$$

$\mathscr{D}$ is the diffusion coefficient of the glycol, and R_0 the ratio of the particle when t = 0.

Additionally, the second order homogeneous kinetic model and the equilibrium limited homogeneous kinetic model were evaluated. In this case, a homogeneous kinetic model that takes into account the reversibility of the monomer-oligomers equilibrium was considered, as shown in Equation (15):

$$-\frac{dC_{PET}}{dt} = k_1 C_{PET}^a C_{EG}^b C_{CAT}^c - k_2 C_{CAT}^C C_{BHET}^d \tag{15}$$

Assuming constant concentrations of both the catalysts and the glycol, and a first order reaction rate with respect to all the species implied, we obtain the final Equation (16):

$$-ln\left(1-\frac{X}{X_e}\right) = \frac{k_1^{\text{Å}}}{X_e}t \tag{16}$$

The detailed mathematical development of these expressions can be found in [48] and [49], respectively. In summary, the four models fitted to the kinetic data are listed in Table 2 and the best model was selected based on the coefficient of determination (R^2) value:

2.6. Carbon footprint calculations

The calculation of the Carbon Footprint (expressed as kg CO_2-eq per kg recycled PET) is based on a potential flow chart of the investigated depolymerization process, comprising the pretreatment, which included shredding, washing, float-sink separation, and drying. Additionally, the glycolysis process itself, based on lab conditions, downstream processing of the used solvents, i.e., purification using a distillation process, and the crystallization of BHET are also considered based on enthalpy calculations. Given that solvent recovery and applied solid–liquid ratio are the key factors in environmental impact assessments of chemical recycling processes, as identified in previous studies, a sensitivity analysis is performed for these two process parameters [50,51]. Data for the depolymerization process were adapted from the results obtained at lab-scale. Energy calculations are based on the specific heat capacity and the latent heat of vaporization of the suggested solvents. As benchmark scenario, incineration of the polymer and substitution of the incinerated plastics by virgin plastics is assumed. Moreover, the current scenario is compared to the solvent-free glycolysis with TBD as catalyst, taken from Fukushima et al. [12]. For both cosolvent-free and cosolvent assisted depolymerization, ethyl acetate was used as crystallization solvent instead of water due to the low solubility of the monomer in this solvent as well as its lower boiling point (77.10 °C at 1 bar) which facilitates its separation by distillation from the EG [52,53]. Additionally, as no catalyst regeneration step was included and during the reaction the TBD is protonated and therefore most of its catalytic activity is lost, the species was considered as residue for both scenarios. Further research about the regeneration and recirculation of the catalysts in the system is required, although this is out of the scope of the present study. A detailed flowsheet is presented in Fig. 9a, and a detailed inventory is presented in Table S4. The carbon footprint for the different processes was extracted from the Ecoinvent database v3.1 in OpenLCA 1.9.

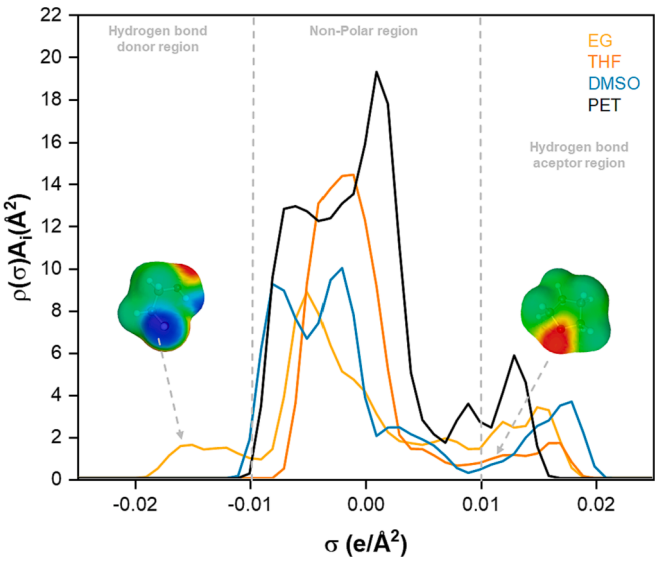

Fig. 2. Superimposed σ-profiles of PET with THF as one of the most optimal solvents based on γ at 65 °C, a solvent with low affinity as DMSO and one with no affinity at this conditions as the glycol. σ-values higher than 0.01 e/Å^2 show electron donor abilities and below 0.01 e/Å^2 show electron acceptor abilities and values in between indicate non polar interactions.

3. Results and discussion

3.1. Theoretical tools for solvent selection

We used the Hansen Solubility Parameters (HSP) and COSMO-RS to identify and understand the nature of the intermolecular interactions between various organic solvents including polar, non-polar, and hydrogen-bonded liquids with PET. Proton-donor solvents were excluded as these species could inhibit the glycoxide ion by the action of the "cage effect" [54]. Furthermore, molecular solvents without chemical inertness to the strongly basic environment of the reaction were not considered. A total of 21 solvents were selected for analysis (see Table S1).

A system composed by polymer–solvent pairs with similar HSP are expected to be mutually soluble. However, for PET-solvent pairs, these parameters have certain limitations as this method was developed mainly for amorphous, non-polar polymers, leading to non-accurate predictions for semicrystalline and polar materials [41]. Considering this, solvents with a Ra distance < 11.0 MPa$^{1/2}$ are considered to have the potential to interact with PET [35]. Based on HSPs, the molecular solvents with the highest affinity towards PET are cyclic ketones and ethers, followed by the family of the strongly dipolar aprotic solvents. Moreover, no significant interaction will exists among the material and non-polar solvents such as cyclohexane as well as with protic polar solvents such as alcohols, ethylene glycol and water. Some of the solvents selected were ketones, such as cyclopentanone (Ra = 1.93), acetophenone (3.75), and 4-methyl 2-pentanone (5.98); the acetal 1,3-dioxolane (7.29); linear and cyclic ethers like tetrahydrofuran (8.17)

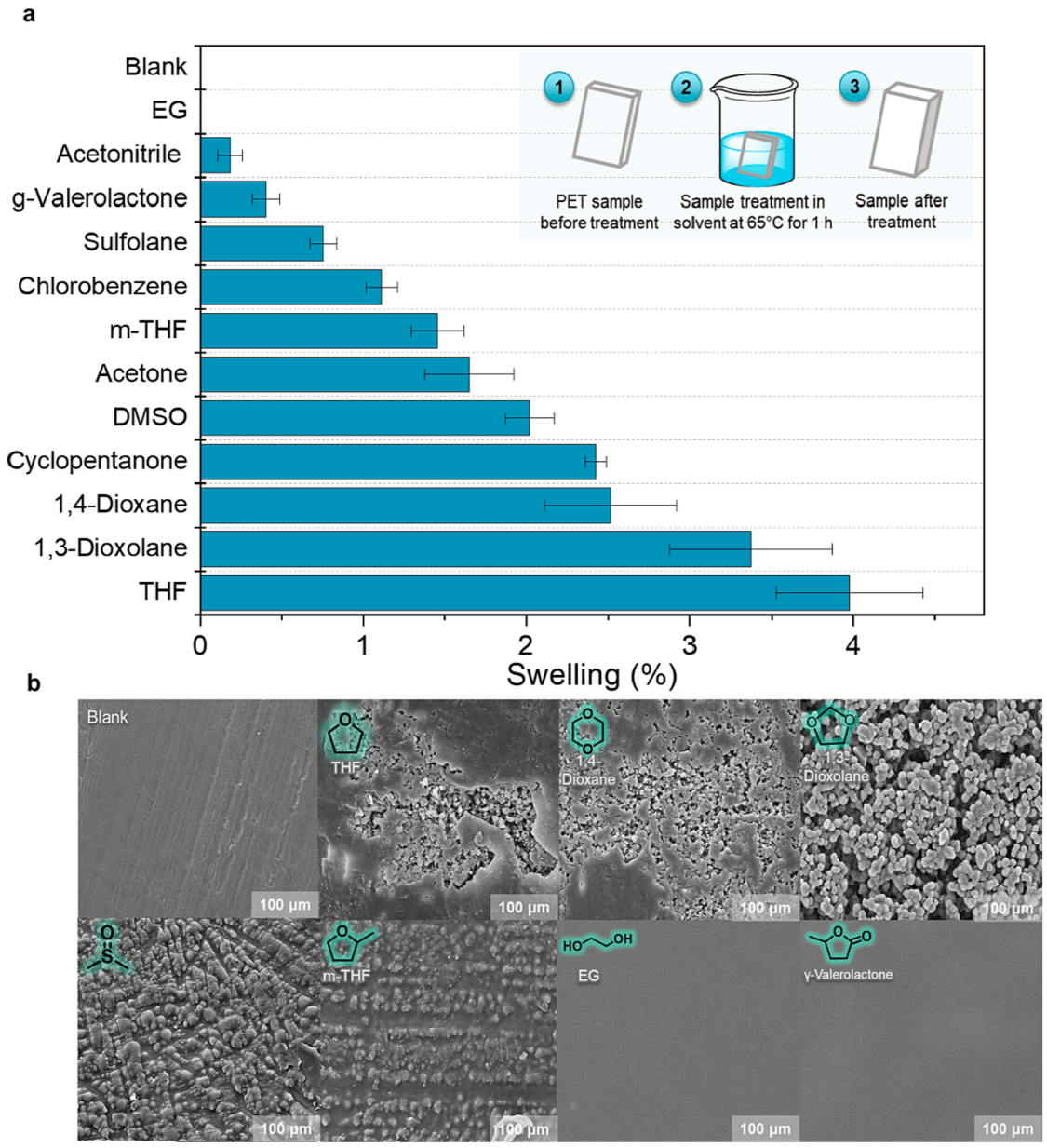

Fig. 3. Experimental validation of the interaction among PET and solvents detected by theoretical approaches. (a) Solvent uptake (swelling) experiments of PET model particles in contact with the solvents evaluated as compatible using theoretical approaches (b) SEM microtomes of the changes of the morphology on the surface of the model particles.

or 1,4-dioxane (10.52); and dipolar aprotic solvents like DMSO (7.31) and acetonitrile (9.42). The typical halogenated solvents were discarded in this first analysis due to their low boiling point and EHS issues, despite their Ra value were within the established threshold [55]. Carbonates and esters like methyl acetate (8.68) and ethyl acetate (9.32) were also omitted due to their lack of chemical inertness in the presence of the basic catalyst [56].

Furthermore, the σ-profiles of solvents and PET were calculated at 65 °C as ceiling temperature value close to the boiling point of THF, being the most volatile species found in the HSP based pre-screening stage. These profiles serve as valuable indicators of the system's affinity to a surface of polarity σ, which, in turn, provides insights on the most plausible interactions between macromolecules themselves, as well as with solvents (See Fig. 2) [57]. According to this method, PET has most affinity towards hydrogen-bond donor solvents that have the ability to interact with the ester moiety such as m-cresol, chlorophenol, chlorinated, and fluorinated acetic acids [58,59]. From the σ-profile of PET, we can infer that the main interactions of the polymer with solvents are those of non-polar or dispersive nature, such as solvents allowing π-π stacking, as well as the ones derived from intermolecular H-bonds. These H-bond interactions occur at the oxygen of the basic carbonyl group of the ester moiety acting as an electron donor in presence of proton bond-donor solvents, which is the case for cresols or fluorinated acetic acids. However, this interaction seems not to be relevant for strongly hydrogen-bonding solvents, such as EG, ethanol or methanol, since the polymer is insoluble in these solvents. Moreover, weak interactions may exists with hydrogen-bond acceptor solvents and the slightly acidic protons associated to the carbons of the ethylene repetitive unit (Fig S1). Most of the solvents selected in the first screening process are proton acceptors. Therefore, we hypothesize that the main interactions existing between the material and these species are of dispersive nature and with the hydrogens of the ethylene moiety.

On the other hand, the activity coefficient (γ) of PET in the binary mixture with the solvents selected was calculated using the

Table 3
Solvents found to be compatible with PET using theoretical tools alongside the induced T_g.

Solvent	$T_{gInduced}$ (°C)	T_g (°C)	Swelling (%)	Activity coeficient (γ)	Molar Volume (cc/mole)
THF	34	79	3.97 ± 0.4	0.97	81.7
1,3-Dioxolane	37	78	3.37 ± 0.49	0.96	69.9
1,4-Dioxane	40	77	2.51 ± 0.41	0.92	85.7
m-THF	44	78	1.45 ± 0.16	1.02	100.2
DMSO	45	76	2 ± 0.15	2.72	71.3
Cyclopentanone	47	77	2.42 ± 0.06	0.88	89.1
EG	None	75	0	2.9	55.8
Blank	None	79	——	——	——

thermodynamic data obtained by COSMO-RS. Our computations show that the solvents with the strongest interaction with the material expressed in terms of the activity coefficient value are the ketones cyclohexanone (γ = 0.862) and cyclopentanone (0.882); the ethers 1,4-dioxane (0.919) and THF (0.970); and the acetal 1,3-dioxolane (0.967) (Table S1). This result is in accordance with the findings obtained during the calculation of the Ra distance using the HSPs, with the exception of the high γ values associated with polar aprotic solvents like acetonitrile (2.185) and DMSO (2.721), which are as high as the ones observed for the alcohols ethanol (2.593) and methanol (2.903).

3.2. Experimental validation of PET-solvent interaction

3.2.1. Swelling behaviour

Following on the theoretical solvent selection tools employed in the previous section, we focused on the solvents with the highest potential for success and on those with the lowest potential. In this regard, we quantified the degree of swelling of PET in presence of 13 solvents at 65 °C for 1 h in order to confirm either the existence or absence of interactions between the polymer and the liquid. When polymers are brought into contact with a thermodynamically compatible solvent, the liquid impregnates the material by diffusion, leading to its swelling or in some cases/conditions to complete dissolution [60]. During this phenomenon, polymer relaxation occurs at the boundary front induced by the swelling pressure, increasing the chain mobility [37,61]. For the solvents studied, the highest swelling percentage was reported for the samples that were soaked in THF (4 %), 1,3-dioxolane (3.4 %), and 1,4-dioxane (2.51 %). (Fig. 3a) On the other hand, the swelling of PET in cyclopentanone (2.4 %) was much lower in comparison to THF, although we expected a better behaviour based on the HSPs and COSMO-RS (Ra and γ) calculations that suggested a higher interaction between the cyclic ketone and the polyester. The lower boiling points and molecular volumes of the cyclic ethers and the acetal can explain the better performance of these species in comparison to the ketone to achieve polymer swelling. This phenomenon is strongly influenced by solvent diffusion, which is dependent on the temperature and the solvent molecular size (see Table 3) [24].

On the other hand, no swelling was reported in the samples treated with EG. Therefore, we conclude that when PET is soaked with the glycol at temperatures below its T_g, limited transport of solvent occurs into the polymer matrix. This is in accordance with the information obtained by applying both theoretical approaches, as for this solvent the Ra value was equal to 21.82 and the γ value to 5.977, which are considerably higher than those of other solvents evaluated. Moreover, it was observed that the PET samples remain unaltered by EG and retained its transparency in contrast to the samples treated with the other solvents. The samples treated with these solvents exhibited haziness after drying the remaining liquid from the surface of the particle after the treatment (See Fig. S3). This behaviour of the material can be used as a qualitative approach to evaluate its competitivity of solvents in a simple way.

3.2.2. Morphology and changes on thermal properties

Additionally, the morphology of the PET samples was examined via SEM after treatment with some of the solvents tested during the swelling experiments. This is specifically relevant to understand the morphological changes occurring due to the uptake of the solvents. We observed the change from a smooth and clear texture of the PET particle surface to a cavitated one when the sample was soaked in the THF and 1,3-dioxolane (Fig. 3b). Longer immersion times in some solvents had the effect of causing uniform and more pronounced cavitation over the surface (Fig. S4). Although the cavitation of the sample surface was uniform in those treated with the acetal, in the case of those immersed in the cyclic ether a more localized cavitation was detected. This can be attributed to the presence of defects on the plates that appeared during the processing of the material. In the samples treated with DMSO and m-THF rugosities appeared on the surface texture, showing a milder effect than dioxolane and THF. Furthermore, no changes were observed in the samples treated with ethylene glycol and γ-valerolactone. Similar results were obtained by Desai et al. [62] and Alonso et al. [63] after treating amorphous PET films with 1,4-dioxane and DCM at different temperatures and times. They concluded that changes in the surface morphology were a direct consequence of the PET solvent induced crystallization coming from the penetration of the compatible, low molecular weight liquids into the polymer matrix after plasticisation [64]. The solvent induced crystallization phenomenon was confirmed when the presence of spherulites was detected in the samples treated in 1,3-dioxolane and DMSO using Polarized Light Optical Microscopy (PLOM) (see Fig. S5). In the sample treated with DMSO, the spherulites formed were significantly smaller than those observed in the 1,3-dioxolane treated samples. This phenomenon was attributed to the higher molecular mobility promoted by the cyclic acetal in the polymer matrix due to the higher affinity of this solvent towards the material in comparison to the DMSO. Additionally, the solvent induced crystallization was also measurement by calculating the cold crystallization enthalpy (ΔH_{cc}) of model PET samples treated in the solvents. In Fig. S6 it is observed that in THF, 1,3-dioxolane and 1,4-dioxane the cold crystallization peak disappeared and in m-THF, DMSO and cyclopentanone as the area below the ΔH_{cc} decreased in comparison to the blank and the sample exposed to EG.

Plasticisation was correlated to the decrease of the glass transition temperature ($T_{gInduced}$) measured in the wet specimens, which is caused by the additional free volume induced by the solvent [65]. To study this effect, PET model samples were treated with some of the best solvents and with EG, considered as the one with no affinity towards PET at 65 °C. Again, cyclic ethers and acetal have been found to exhibit higher levels of reduction on the PET T_g, followed by DMSO and cyclopentanone, respectively (Table 3). Moreover, from the results obtained using DMTA in the sample exposed to THF and the blank, we confirm the presence of a second T_g at 33 °C caused by the plasticization of the material by the solvent (See Fig. S7). The effect of THF, 1,3- dioxolane, m-THF, DMSO and EG on the model PET samples at different times was followed by FTIR as well (See Fig. S9). No changes were observed on the spectrum from the original sample in comparison to the sample treated with solvents besides an increase of the transmittance percentage on samples treated with THF and 1,3-dioxolane. No shifts were noted in the signals associated to the aromatic moiety and the new signals observed were assigned to trace solvents remaining in the sample.

Based on our approach, cyclic ethers, acetals and cyclic ketones were found to be the ones with the highest affinity towards the amorphous PET specimens from their solvent uptake as well as from the changes of the morphology and thermal properties. Some of these solvents were tested in the glycolysis and the reaction performance of these systems was compared to those carried out in solvents with the worst interaction

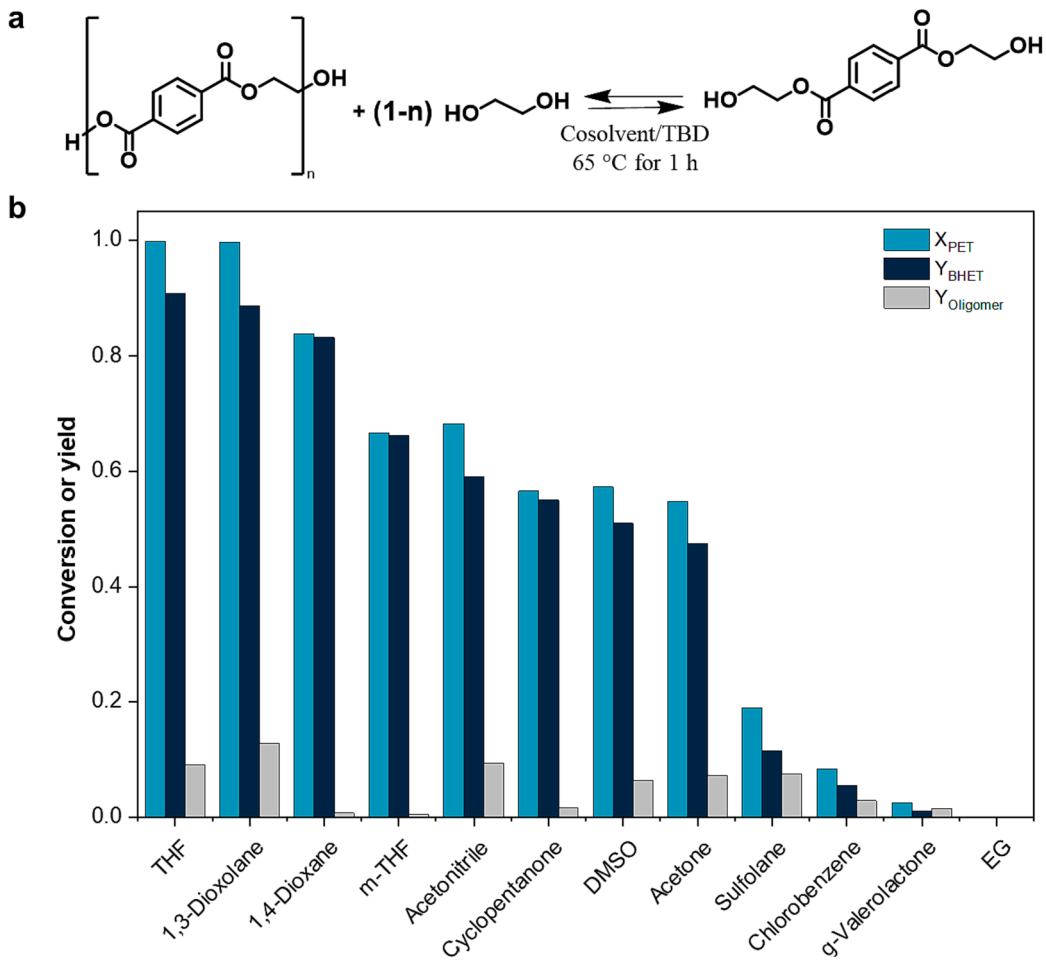

Fig. 4. (a) Glycolysis reaction scheme. (b) PET conversion and product distribution after 1 h of PET glycolysis with and without co-solvents at 65 °C using TBD as catalyst. The molar ratios of EG, co-solvent, and catalyst to PET monomer were adjusted to 3, 14, and 0.1, respectively.

with the material in order to prove their effect on the reaction conditions.

3.3. Effect of co-solvent in the PET glycolysis

3.3.1. Solvent testing

To assess the action of cosolvents in the glycolysis reaction, 1 equivalent (eq.) (1 g) of PET flakes were added to the liquid solution composed by 15 eq. (5 g) of EG and 0.1 eq. (70 mg) of TBD as catalyst. The system was heated up to 65 °C for 1 h and then used as reference. The amount of EG was fixed in 15 eq. to guarantee the soaking of all PET flakes in the flask. For the cosolvent effects studies, 1 eq. of PET flakes were treated in 14 eq. of the solvents considered as the best and worst in the screening. 3 eq. of EG and 0.1 eq. of TBD were used in all the cosolvent trial experiments. In Fig. 4b, it is observed that at 65 °C no reaction occurs when only EG is present in the liquid phase of the system. However, when THF and 1,3-dioxolane were added, complete depolymerization of PET was attained in 1 h. The latter clearly indicates that the swelling of the polymer in the co-solvent facilitates the migration of the nucleophile and the catalyst into the polymer matrix by increasing the diffusion of both species and allowing a better access to the ester moiety (the active site). Additionally, a higher monomer yield was obtained in THF. This can be attributed to the higher molecular movement caused by the lowering of the T_g induced by THF, as well as to the lower boiling point of the solvent, which is close to the reaction temperature and facilitates the mass transfer between the polymer in the solid phase and the liquid phase. In contrast to the excellent performance achieved with THF, total conversion of PET was not achieved in 1,4-dioxane and m-THF, although the three solvents present similar polarity, density, and viscosity. Moreover, a higher solvent uptake was reported for THF in comparison to m-THF during the swelling test. We attribute this behaviour to the higher molar volume of m-THF (100.2 cc/mole vs. 81.7 cc/mole of THF) as well as to the higher boiling point of the solvent, which reduces its diffusion into the polymer and make it a bad carrier for the nucleophile and the catalyst [66].

Furthermore, the boiling point of dioxane is higher in comparison to THF although the MV is lower. The last indicates that the reaction rate of PET glycolysis below its T_g is strongly affected by mass transfer phenomena as well as by the affinity of the material towards the solvent. Therefore, parameters such as the molar volume and boiling point of the cosolvent are important to obtain complete PET degradation and high monomer yield. We observed the same trend in the systems with ketones as cosolvents. For instance, the reaction in cyclopentanone exhibited a slightly higher degree of conversion compared to the system in acetone, although the monomer yield was better in the cyclic ketone. From this, we can infer that no higher conversion was reached in cyclopentanone as consequence of the higher viscosity and other physical properties of the solvent that affect the mass transfer of the glycol and the catalyst towards the solid [57]. A similar behaviour was observed for the dipolar aprotic solvents. A higher conversion of 0.68 was obtained in acetonitrile compared to 0.57 in DMSO, although the intake of the last solvent by the material is higher. However, the boiling point and viscosity of acetonitrile are by far lower than the ones of DMSO, which can help to a faster mass transfer between phases. Additionally, the performance of the acetonitrile system can be correlated to the interaction of the solvent with the glycol and the catalyst in the liquid phase as the two solvents

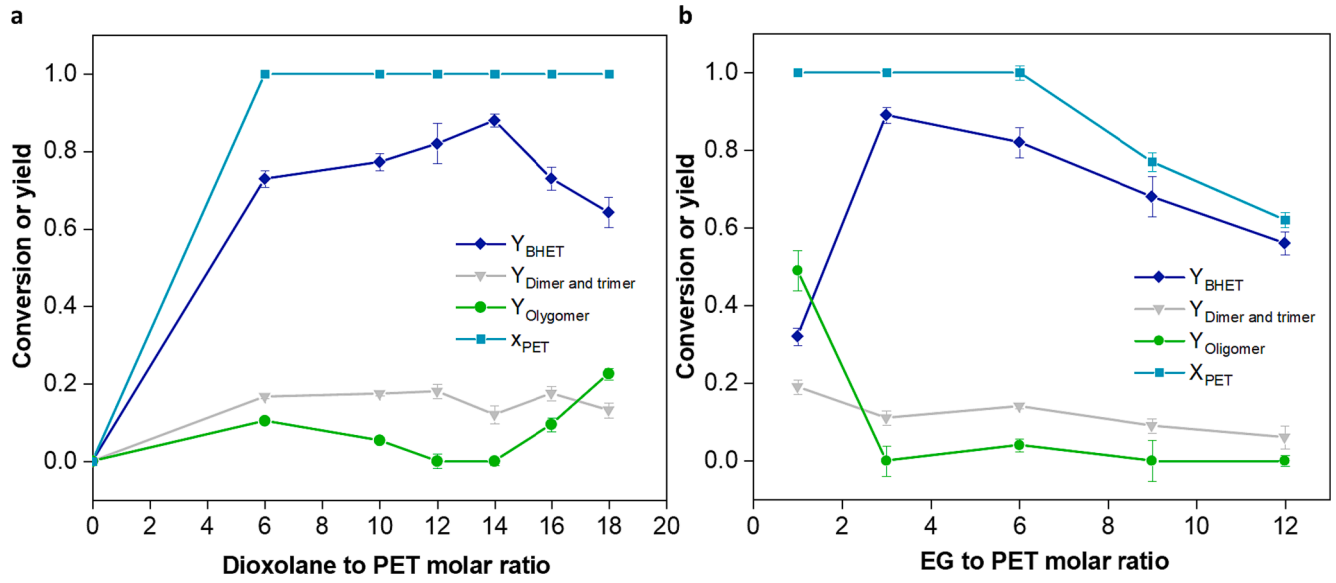

Fig. 5. (a) Effect of cosolvent to PET ratio and (b) effect of EG to PET molar ratios on the PET conversion and glycolysis products distribution.

Table 4
Fitted models to the kinetic data obtained from the reactions assisted by some of the evaluated co-solvents. $\acute{k}$ is equivalent to K_c and K_d for HE_1 and HE_2, respectively. For HO_1, $\acute{k}$ is $k_1^{\AA}$.

Solvent	Best fit model	$\acute{k}$
1,4-Dioxane	HO_1 ($R^2 = 0.994$)	0.03965
	HO_2 ($R^2 = 0.993$)	0.03401
	HE_1 ($R^2 = 0.945$)	0.0081
	HE_2 ($R^2 = 0.921$)	0.0126
1,3-Dioxolane	HO_1 ($R^2 = 0.996$)	0.1103
	HO_2 ($R^2 = 0.993$)	0.09682
	HE_1 ($R^2 = 0.816$)	0.0081
	HE_2($R^2 = 0.751$)	0.0113
m-THF	HO_1 ($R^2 = 0.936$)	0.01827
	HO_2 ($R^2 = 0.971$)	0.01514
	HE_1 ($R^2 = 0.989$)	0.0051
	HE_2 ($R^2 = 0.921$)	0.0089
Cyclopentanone	HO_1 ($R^2 = 0.914$)	0.04832
	HO_2 ($R^2 = 0.855$)	0.02094
	HE_1 ($R^2 = 0.802$)	0.0037
	HE_2 ($R^2 = 0.784$)	0.0066
DMSO	HO_1 ($R^2 = 0.936$)	0.01425
	HO_2 ($R^2 = 0.978$)	0.01102
	HE_1 ($R^2 = 0.9887$)	0.0037
	HE_2 ($R^2 = 0.9863$)	0.0067

combined form an isodielectric system. Future research could examine this last effect more in depth in the low temperature PET glycolysis.

3.3.2. *Effect of cosolvent molar ratio on the reaction*

Additionally, the effect of cosolvent molar ratio on the PET conversion and monomer yield is studied. For these experiments, we selected 1,4-dioxolane instead of THF as cosolvent given that it is classified as green solvent in the last GSK's solvent sustainability guide as well as it was reported to be non-toxic, eco-friendly and non-carcinogenic [26,67]. Moreover, due to the low point of the solvent (75 °C at 1 bar) it is easy to separate from the ethylene glycol during the purification of the reaction crude. As it was already observed, no conversion of PET is obtained when no cosolvents were added to the system at 65 °C (Fig. 5a). However, when the molar ratio of dioxolane to PET is equalled to 6, the flakes solubilize entirely in 1 h, and a BHET yield of 73 % is achieved. Moreover, when the cosolvent-to-PET-ratio increases, the monomer yield is higher as well, reaching a maximum of 88 % when a molar ratio of 14 was set. Above this value, the oligomer by-product amount produced became higher, which we attributed to the dilution of the nucleophile, as high excess of glycol is required to push the equilibrium towards the formation of monomers and to reduce the formation of by-products.

Fig. 5b indicates that the excess concentration of glycol must be carefully monitored to suppress any negative effect of the cosolvent in the reaction. When the EG-to-PET-ratio is as high as 12 in a fixed cosolvent to PET ratio of 14, the action of the dioxolane is less relevant as conversion of PET falls from 1 to 0.7 while no oligomer by-products are detected. We can attribute the lower formation of oligomer to the higher concentration of the glycol as more of the nucleophile is available to the break the short-chain oligomers present in the liquid phase. Based on this, we conclude that both molar ratios evaluated are crucial to get the highest yield possible of BHET. The cosolvent-to-PET ratio needed to totally decompose PET is 14, and the optimal EG-to-PET ratio to achieve the maximum quantity of monomers is 3.

3.3.3. *Cosolvent effect on the reaction kinetics*

Two heterogeneous as well as two homogeneous kinetic models were fitted to the data obtained from the glycolysis in several cosolvents in order to study the effect of these in the reaction kinetics (see Table 4). The HO_1 kinetic model fits the most accurately for the systems in which complete PET conversion and the highest BHET yields were reached (Fig. 6a) However, for DMSO and m-THF, an induction period of 8 min occurs, prior to the increase in the BHET molar fraction. The solvents that exhibit relatively low reaction yields are most accurately modelled by the contracting geometry and the diffusion model. The behaviour of the reaction in the presence of solvents with the highest affinity is explained by the presence of the swollen layer on the PET particles surface, in which the polymer chains are relaxed and more exposed to nucleophilic attacks (Scheme 1). In parallel to the relaxation of the polymeric chains as consequence of swelling, the TBD catalyst activates the oxygen of the carbonyl group in the ester group and making it more prone to suffer nucleophilic attacks as well as generates the glycoxide ions through hydrogen bonding interactions [12]. Additionally, we can infer that the boundary layer between the liquid bulk for the systems composed by the glycol and the cyclic ethers and acetals and the solid particle is thinner, which improves the mass transfer at lower temperatures. Additionally, the presence of hydrogen-bond acceptor cosolvents in the liquid phase may reduce the self-association effect between the free glycoxide ions and the glycol molecules, increasing the concentration of free ions available for the reaction [68].

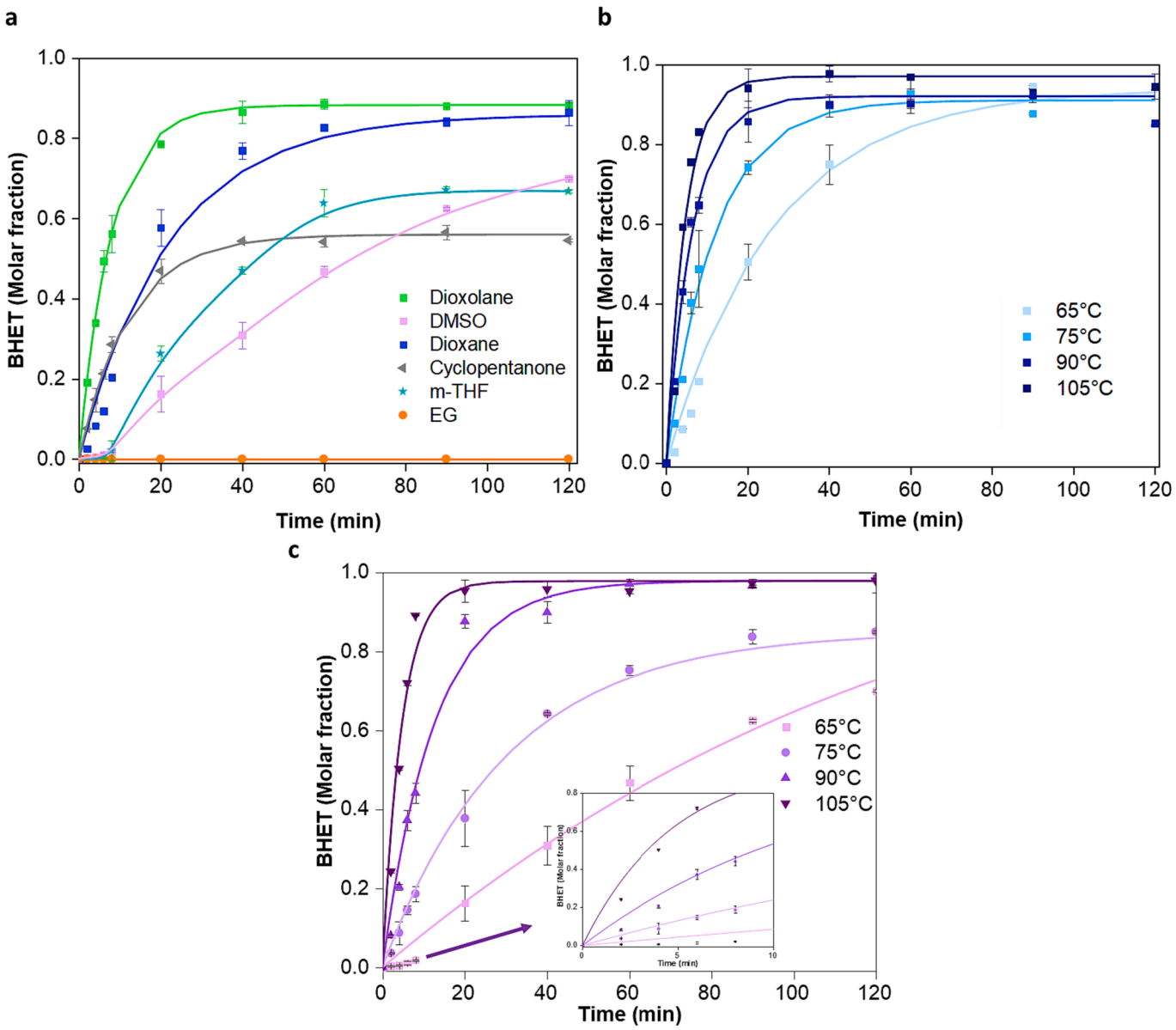

Fig. 6. (a) Kinetic experiments for the cosolvent assisted glycolysis in different solvents at 65 °C for 2 h, (b) Kinetic experiments in dioxane. At higher reaction temperatures, BHET yield increases faster. Then, repolymerization occurs if the reaction last more than one hour. (c) Kinetic experiments for the DMSO assisted glycolysis at different temperatures. When the reaction temperature increases, the delay at the first minutes of reaction disappears.

Moreover, in order to study the effect of temperature on the reaction kinetics of the heterogeneous-like systems, glycolysis in 1,4-Dioxonae and DMSO as cosolvents was carried out at temperatures within the T_g interval (75 °C) and above (90 °C and 105 °C). Both solvents were selected as their BP values are within or close to the highest reaction temperature evaluated. In Fig. 6b we observed that in the cyclic ether, BHET yield (and therefore the PET conversion) increases from 0.75 after 40 min of reaction at 65 °C to 0.97 at 105 °C. However, after one hour of reaction at 90 °C and 105 °C the BHET yield decreased as the dimer/trimer concentration increased as consequence of the monomer repolymerization. Furthermore, only the data obtained from 0 to 60 min were considered for the kinetic model evaluation as the four model selected do not consider the BHET polymerization. Considering this, the HO_1 kinetic model predicted the best the behaviour of the dioxane-assisted glycolysis reaction at all the temperatures tested. On the other hand, in Fig. 6c it can be observe that both the conversion and the kinetics change by increasing the reaction temperature from a heterogeneous like system to a homogeneous like one. Ueberreiter et al. found in their studies regarding the dissolution of Poly(methyl methacrylate) in pure solvents and binary blends that the rate of penetration of the small molecule solvents increased with higher temperatures as the chains can relax more readily [69]. Based on this and the additional data, we suggest that the effect of cosolvents in the system can also be better controlled by varying other reaction parameters such as the reaction temperature. In conclusion, the PET glycolysis process can be described by homogeneous and heterogeneous (shrinking core model) models depending upon the studied operating conditions. Understanding the importance in considering the experimental conditions during the modelling of PET depolymerization is an important finding of this study, underscoring the complexity of such processes.

3.3.4. *Crystallinity effect on the solvent assisted PET glycolysis*

Given that our previous research indicates the importance the co-solvent in facilitating mass transfer during the reaction, we also investigate here the impact of the degree of crystallinity in the depolymerization process [70]. The presence of crystallites in the PET polymeric

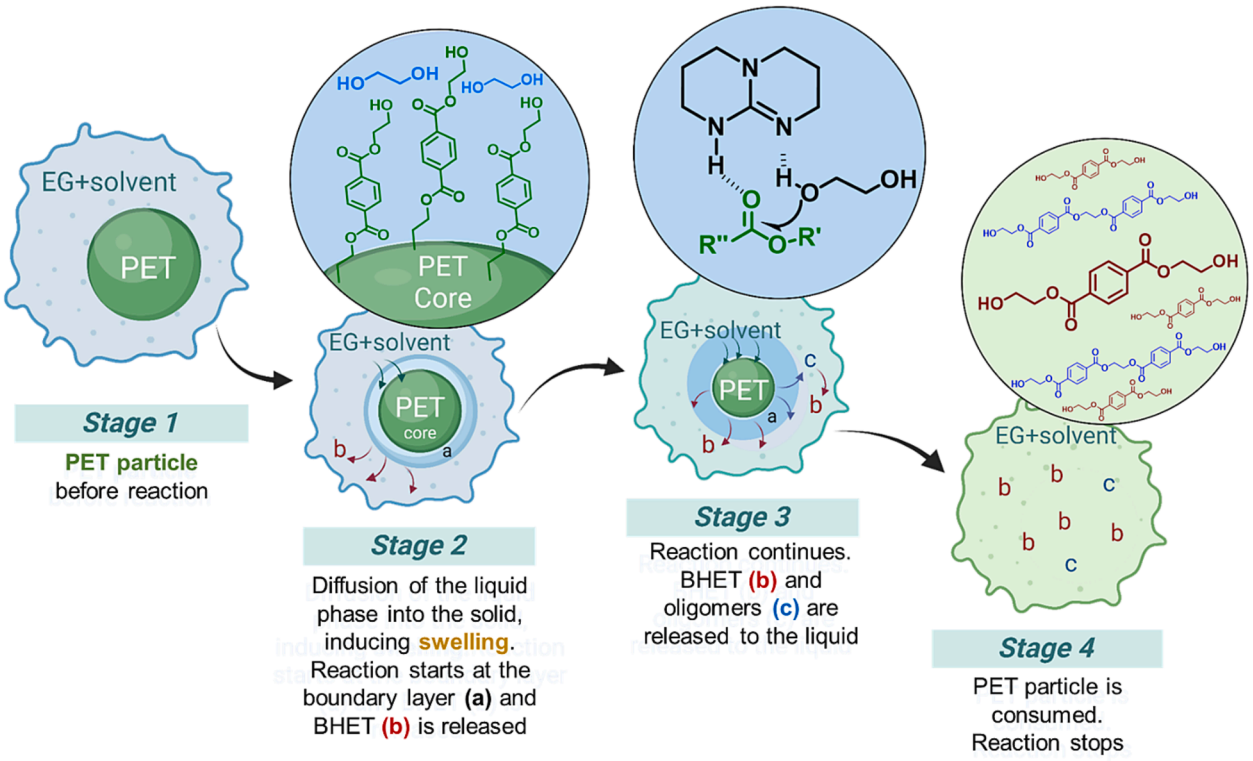

Scheme 1. Mechanism of the Solvent assisted glycolysis mechanism with TBD as catalyst.

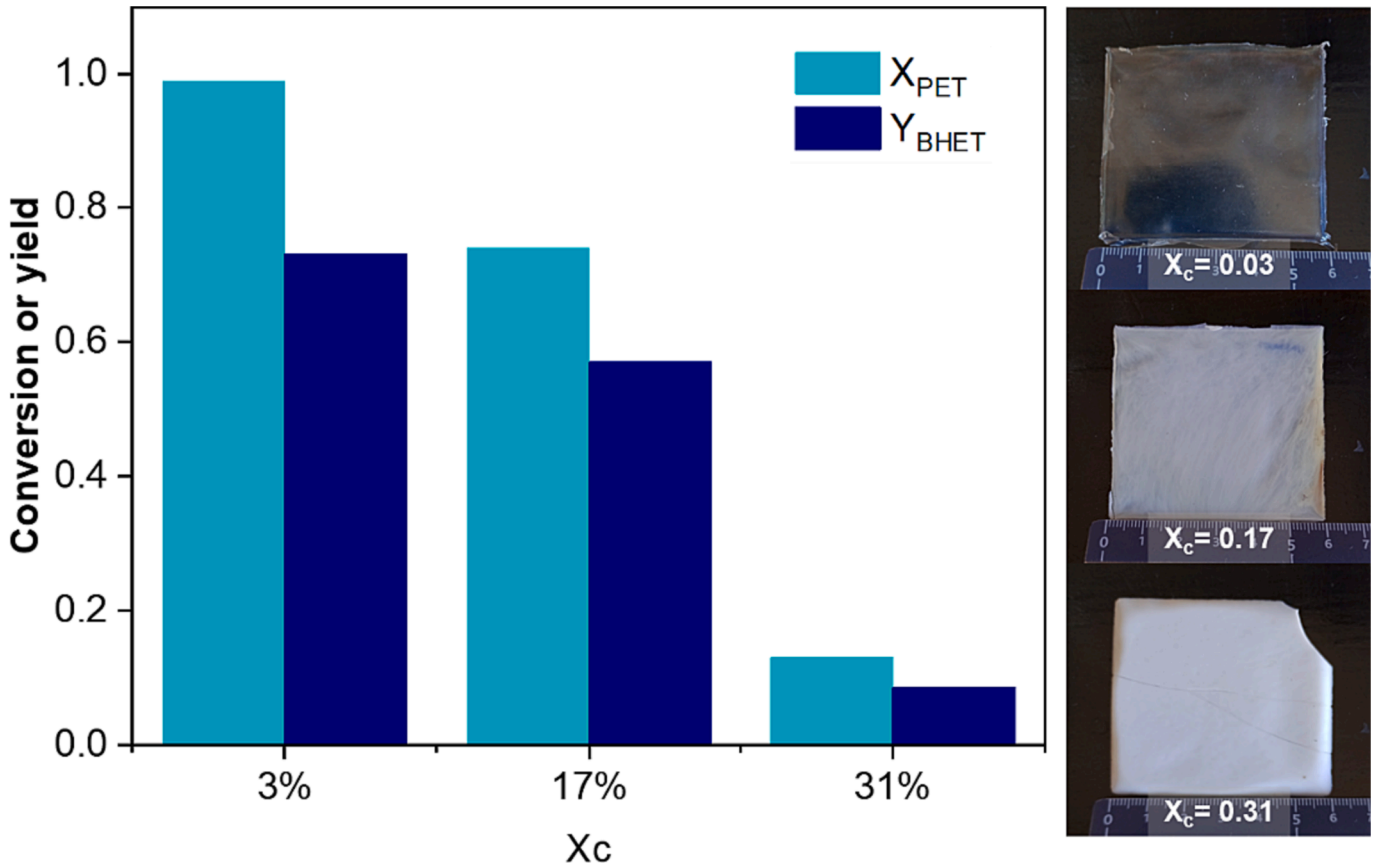

Fig. 7. Evaluation of the effect of the sample crystallinity on the glycolysis reaction. The reaction temperature and time were 65 °C and 1 h, respectively. The PET samples treated had crystalline mass fraction of 0.03, 0.17 and 0.31.

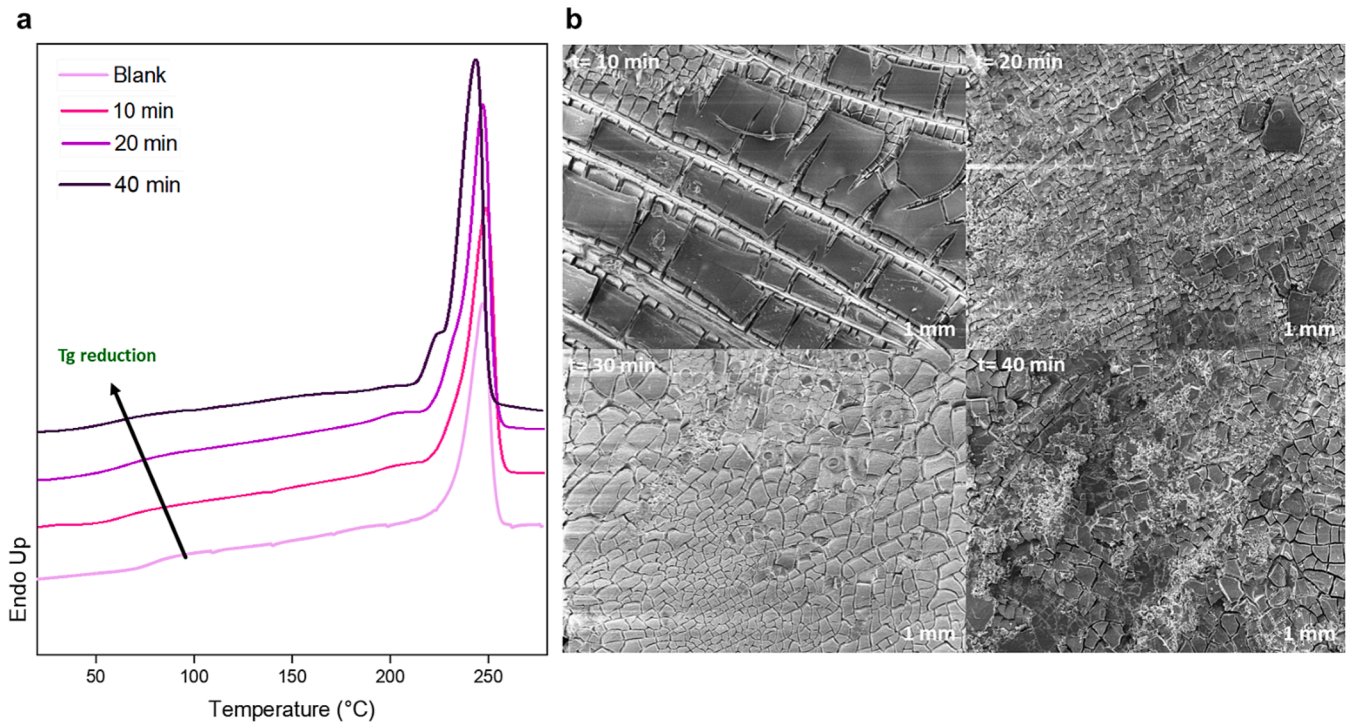

Fig. 8. (a) DSC 2nd scan of PET sample at different reaction times. (b) Changes of the morphology of PET sample surface at different reaction times.

matrix protects the ester reactive sites from suffering attacks and reduce the diffusion of fluids in the material by acting as crosslinkers, reducing the free volume in the amorphous fraction (See Fig S17). Therefore, polymers with very low crystal mass fraction degrade faster than their crystalline counterpart [71]. In order to study the effect of crystallinity degree on the solvent-assisted PET glycolysis, PET plates of different crystal mass fraction were made following the same procedure described before for the model samples but this time in order to reach the desired crystallinity for the samples we followed the procedure described in [72]. Subsequently, we cut 1 g of each PET plate into pieces with approximately the same dimensions as the ones of the PET bottles. The reactions were run in 14 eq. (1),3-dioxolane as co-solvent, 0.97 g of ethylene glycol and 70 mg of TBD. The reaction temperature was 65 °C and lasted 1 h (Fig. 7a).

Following our expectations, the flakes derived from the PET plate with 3 % of crystal mass exhibited nearly complete conversion under the applied reaction conditions; however, the BHET yield was lower compared to the one obtained when bottle flakes were treated. We mainly attribute this to the higher thickness of the amorphous flakes obtained from the virgin plate, which affects the mass transfer in the axial direction from the plate surface to the liquid phase. Additionally, the flakes having a crystal mass of 17 % did not completely depolymerize, and those having a crystal mass of 31 % presented almost no change at the end of the reaction time (Fig. 7b). From this, we confirmed the effect of the solvent as carrier of the glycol and catalyst into the free volume available in the amorphous phase of the solid. Therefore, the higher the crystallinity of the sample is, the less is the free volume available.

3.4. Depolymerization of highly crystalline PET samples using solvent assisted glycolysis

While the initial optimized conditions of 65 °C were suitable for the depolymerization of amorphous PET, when suing these conditions with a semi crystalline PET (31 % of crystalline mol fraction), negligible depolymerization were obtained. In order to verify if the glycolysis of highly crystalline PET samples could be enhanced in the presence of solvents, pellets of virgin material with a crystal fraction of 0.41 were used. In order to increase the mass transfer, we have seen that with DMSO we can move from a heterogenous process to a homogeneous process just by raising the temperature. Therefore we perform the depolymerization reaction at 140 °C in the presence of DMSO and anisole, two of the best solvents from previous section with high boiling points. We compare the depolymerization process with the solvent free depolymerization process (Fig. S20 and S21). After 8 h, when most of the pellets disappeared in the systems with DMSO and anisole, we did not observe any significant change in the sample containing only ethylene glycol. In fact, we measured a PET conversion of 12 % in the system with only EG and up to 94 % was obtained in DMSO and anisole. Unfortunately, the BHET yield was much lower compered to the amorphous systems with 38 % and 63 % of BHET respectively. We can conclude that glycolysis of crystalline PET is possible at temperatures as low as 140 °C but in this case, further investigation will be needed to enhance the BHET yields.

Taking into account the great impact of the crystallinity in the glycolysis, we can assume that PET depolymerization is not a random event. Ester bonds close to the particle surface and in the amorphous phase will break first than the bonds in the crystalline fraction. To confirm this phenomenon we assume that as the reaction progresses in time, the part of the material that is not able to crystallize will be consumed first, increasing the proportion of the total crystal mass fraction. To corroborate this fact, DSC analysis was performed at t = 0 and after 40 min of reaction in the sample containing 31 % crystallinity. In Fig. 8a is observed that the crystal mass percentage increased slightly from 31 % at time 0 to 37 % after 40 min of reaction. The increment can be attributed to the disappearance of the amorphous phase during the reaction which also allows shorter chains present in the remaining solid to crystallize.

In order to corroborate this reorganization, SEM images were taken at different reaction times (Fig. 8b)In Fig. 8b we observe the changes on the morphology of the model particle surface along the reaction. At 10 min, the particle surface presents a three-layered structure. Then, along the advance of the reaction, the surface is fragmented into more little pieces until almost the end of the reaction, when the particle is no longer

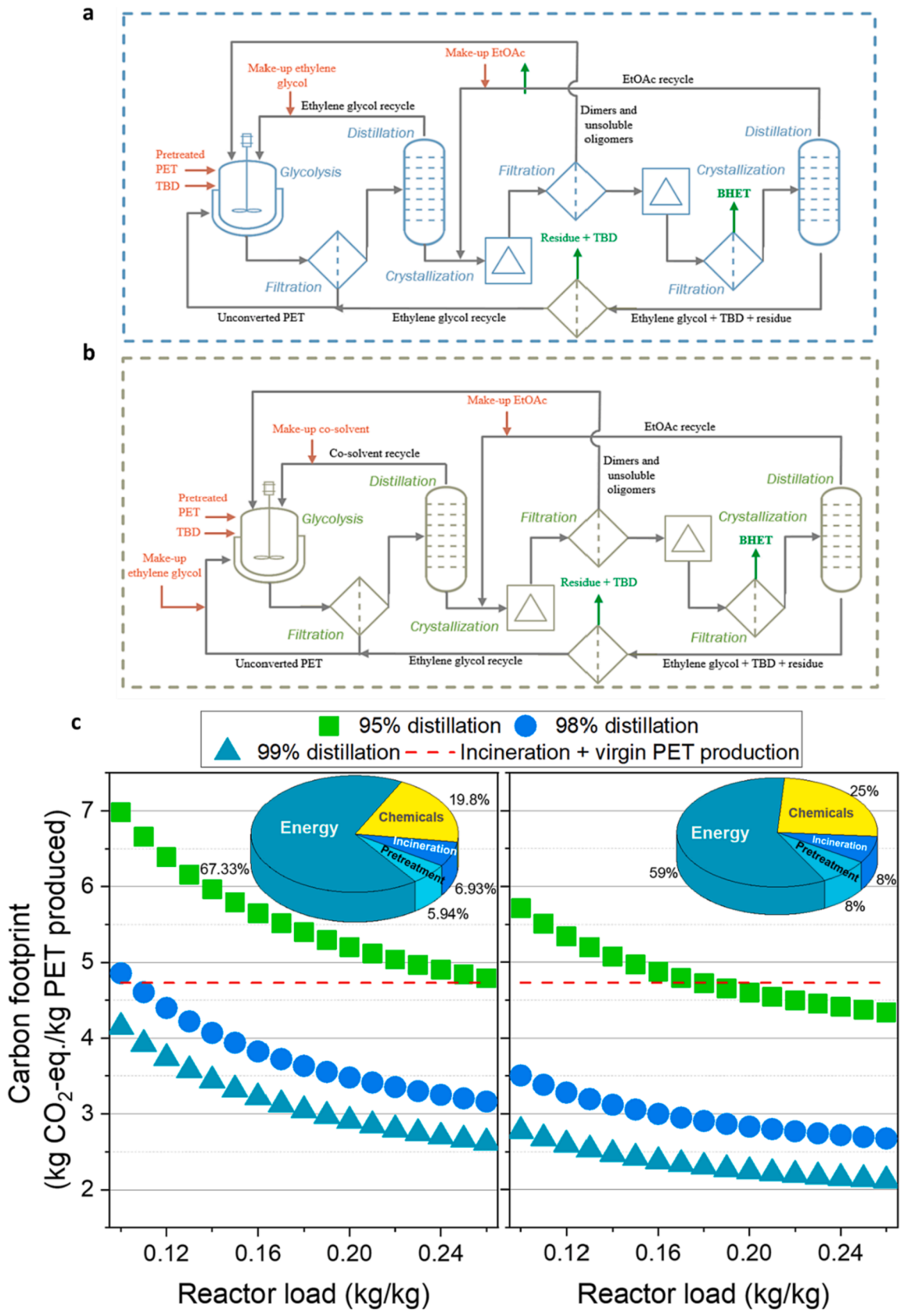

Fig. 9. Process flows of the analyzed scenarios. (a) The glycolysis process used as a reference (without the use of a co-solvent), (b) The new glycolysis process using a1,3-dioxolane as cosolvent and (c) Carbon footprint of both processes calculated in base of the assumptions made for both processes.

visible. The fragmentation of the surface is attributed to the reorganization of the remaining macromolecules into smaller islands conformed by crystalline lamella and amorphous fractions joined by tie molecules.

3.5. Solvent assisted glycolysis Life Cycle assessment (LCA)

Up to this point, we have shown that, especially for the more amorphous PET samples, glycolysis is possible at 65 °C, a temperature below the T_g of the material, in 1 h and using TBD as catalyst. The reaction is possible at these conditions only when a solvent with the capability to swell the material is present as cosolvent. However, in the current context regarding the design of sustainable products and processes, most studies are oriented to the removal of organic solvents from new chemical systems or chemical processes [73]. Recycling of plastics should ideally create environmental benefit compared to the use of virgin material; which can be assessed by LCA or other sustainability assessment methods. In this work, we calculate the carbon footprint of two glycolysis processes based on data obtained at lab-scale and preliminary process flow charts; and compare the impact of these processes with the incineration of PET followed by substitution of the incinerated material by virgin resources. Fig. 8 shows the investigated systems, namely the reference scenario as proposed by Fukushima et al. [12] and the new process presented in this study. The proposed flow charts for the glycolysis of PET comprise the pre-treatment (comprising shredding, washing, float-sink separation, and drying) of PET waste based on [74], the glycolysis process itself (based on lab conditions), the downstream processing of the used solvents (i.e., purification by means of a distillation process), and the crystallization of the BHET.

The results of the carbon footprint analysis are shown in Fig. 9c, indicating the significant influence of the reactor load (i.e., how much plastic is glycolyzed per kg solvent) and the distillation efficiency of the used solvents. In addition, it can be seen that the new scenario (Fig. 7B) has a lower impact compared to the reference scenario (i.e., no co-solvent is used; Fig. 9A) if the same conditions are applied in terms of distillation efficiency and reactor load.

In the case no co-solvent is used, at least a reactor load of 0.11 kg PET/kg solvent has to be used with a distillation efficiency of 98 % to be breakeven with the incineration scenario (i.e., incineration of PET followed by substitution with virgin PET), whereas already carbon dioxide emission can be avoided with the same conditions in the co-solvent scenario. It should be noted that at lab-scale, different reactor loadings are applied for both glycolysis scenarios – namely 0.19 kg PET/kg solvent in the case of the reference glycolysis process and 0.14 kg PET/kg solvent in the case of the new glycolysis process. However, even by applying a lower reactor load (which was done to reduce the viscosity of the solution), an environmental benefit is achieved by the solvent assisted process. This is mainly due to the lower energy demand that is needed to perform the reaction and downstream processing in the case a co-solvent is being used (e.g., the heat capacity of dioxolane is 1.63 kJ/kg.K, whereas the heat capacity of ethylene glycol is 2.42 kJ/kg.K). Hence, it can be seen that energy production contributes to a larger extent to the reference scenario (68 % of the carbon footprint) compared to the new scenario (59 %). This is obviously an important asset of the new method taking into account the global energy transition.

Thus, based on the preliminary process flow, the applied lab conditions and reasonable assumptions (e.g., a distillation efficiency of 98 %), around 20 % carbon dioxide can be saved by the new glycolysis process compared with the reference glycolysis process and around 50 % compared with the incineration scenario. Hence, the developed process can contribute to the European Union's (EU) Green Deal to make the EU's climate, energy, transport, and taxation policies fit for reducing net greenhouse gas emissions by at least 55 % by 2030, compared with 1990 levels [75].

4. Conclusions

This paper aimed at providing a better insight in cosolvent-assisted glycolysis of Polyethylene Terephthalate (PET). First a theoretical prescreening of solvents was done, followed by the study of the interaction or effect of those species in the polymer matrix. Then, the solvents proved to have the strongest interaction with PET were used as cosolvents in the glycolysis in order to get BHET in high yields. Furthermore, the solvent to PET and EG to PET optimal molar ratios were determined and based on the kinetic studies made, we concluded that the reaction behaves as an homogeneous system. Based on these insights, we were able to design a PET glycolysis process based on polar aprotic solvents as carriers for both the ethylene glycol and the TBD catalyst which allows to carry out the reaction at 65 °C in 1 h with total PET conversion and high BHET yield (88 %), conditions never reached before with a single homogeneous catalyst. Dioxolane was selected as optimal cosolvent as the reaction reported the second highest BHET yield when used and due to its greener credentials in comparison to THF. The mild reaction conditions were possible, mainly because of swelling which allows a faster diffusion of ethylene glycol and the catalyst as well as increasing the accessibility to both species to the ester bond. The current work shows that PET glycolysis is a process that depends strongly on mass transport phenomena. Moreover, as diffusion of a liquid phase into a solid is not only dependent of the liquid properties but also the ones of the solid, the effect of the crystal mass fraction on the glycolysis efficiency was studied exposing controlled PET samples of different crystallinity to the same amount of 1,3-dioxolane, TBD and EG at identical reaction conditions. Exploiting the use of solvent we manage to depolymerize highly crystalline samples (up to 41 % of crystallinity) at 140 °C in 8 h. Unfortunately, the obtained BHET yield was lower than in the case of amorphous PET. Yet, for more amorphous samples, the process proposed in this work not only consumes less energy in both the reaction stage and the recovery of the product stage by using the cosolvent, but also emits 20 % less CO_2 than the solvent-free process, indicating the economic and environmental feasibility of the process.

CRediT authorship contribution statement

Emelin Luna: . **Ion Olazabal:** Investigation, Methodology. **Martijn Roosen:** Investigation, Visualization. **Alejandro Müller:** Writing – review & editing. **Coralie Jehanno:** Conceptualization, Writing – review & editing. **Marta Ximenis:** Investigation, Methodology, Writing – review & editing. **Steven de Meester:** Conceptualization, Project administration, Writing – review & editing. **Haritz Sardon:** Supervision, Writing – review & editing.

Declaration of competing interest

The authors declare that they have no known competing financial interests or personal relationships that could have appeared to influence the work reported in this paper.

Data availability

Data will be made available on request.

Acknowledgements

The authors would like to acknowledge the POLYMAT for providing financial assistance to this research. The authors also acknowledge the VLAIO Catalisti Moonshot project Cyclops. Further, the authors would like to express their gratitude towards their colleagues, Dr. Kim Pham, Dr. Sibel Ügdüler, Dr. Nora Aramburu, Dr. Jorge Olmedo, Nicolas Ramos and Tobias De Sommer for their unwavering technical support.

Appendix A. Supplementary data

Supplementary data to this article can be found online at https://doi.org/10.1016/j.cej.2024.148861.

References

[1] I.S. Lase, D. Tonini, D. Caro, P.F. Albizzati, J. Cristóbal, M. Roosen, M. Kusenberg, K. Ragaert, K.M. Van Geem, J. Dewulf, S. De Meester, How much can chemical recycling contribute to plastic waste recycling in Europe? An assessment using material flow analysis modeling, Resour. Conserv. Recycl. 192 (2023), https://doi.org/10.1016/j.resconrec.2023.106916.

[2] Eunomia, PET market in Europe: State of play, 2022. https://petcore-europe.org/news-events/409-pet-market-in-europe-state-of-play-2022.html.

[3] A. Grant, V. Lahme, T. Connock, L. Lugal, How Circular Is PET? (2022). https://zerowasteeurope.eu/library/how-circular-is-pet/.

[4] C. Jehanno, J.W. Alty, M. Roosen, S. De Meester, A.P. Dove, E.Y.X. Chen, F. A. Leibfarth, H. Sardon, Critical advances and future opportunities in upcycling commodity polymers, Nature 603 (2022) 803–814, https://doi.org/10.1038/s41586-021-04350-0.

[5] X.L. Wang, W.L. An, R. Du, F. Tian, Y. Yang, X. Zhao, S. Xu, Y.Z. Wang, Rapid hydrolysis of PET in high-concentration alcohol aqueous solution by pore formation and spontaneous separation of terephthalate, J. Environ. Chem. Eng. 11 (2023), https://doi.org/10.1016/j.jece.2023.109434.

[6] D.D. Pham, J. Cho, Low-energy catalytic methanolysis of poly (ethyleneterephthalate), Green Chem. 23 (2021) 511–525, https://doi.org/10.1039/d0gc03536j.

[7] R. López-Fonseca, I. Duque-Ingunza, B. de Rivas, S. Arnaiz, J.I. Gutiérrez-Ortiz, Chemical recycling of post-consumer PET wastes by glycolysis in the presence of metal salts, Polym. Degrad. Stab. 95 (2010) 1022–1028, https://doi.org/10.1016/j.polymdegradstab.2010.03.007.

[8] S.R. Shukla, A.M. Harad, Aminolysis of polyethylene terephthalate waste, Polym. Degrad. Stab. 91 (2006) 1850–1854, https://doi.org/10.1016/j.polymdegradstab.2005.11.005.

[9] P. Gupta, S. Bhandari, Chemical Depolymerization of PET Bottles via Ammonolysis and Aminolysis, in: Recycling of Polyethylene Terephthalate Bottles, Elsevier, 2019, pp. 109–134, https://doi.org/10.1016/b978-0-12-811361-5.00006-7.

[10] J. Xin, Q. Zhang, J. Huang, R. Huang, Q.Z. Jaffery, D. Yan, Q. Zhou, J. Xu, X. Lu, Progress in the catalytic glycolysis of polyethylene terephthalate, J. Environ. Manage. 296 (2021), https://doi.org/10.1016/j.jenvman.2021.113267.

[11] C. Jehanno, I. Flores, A.P. Dove, A.J. Müller, F. Ruipérez, H. Sardon, Organocatalysed depolymerisation of PET in a fully sustainable cycle using thermally stable protic ionic salt, Green Chem. 20 (2018) 1205–1212, https://doi.org/10.1039/c7gc03396f.

[12] K. Fukushima, O. Coulembier, J.M. Lecuyer, H.A. Almegren, A.M. Alabdulrahman, F.D. Alsewailem, M.A. McNeil, P. Dubois, R.M. Waymouth, H.W. Horn, J.E. Rice, J. L. Hedrick, Organocatalytic depolymerization of poly(ethylene terephthalate), J. Polym. Sci. A Polym. Chem. 49 (2011) 1273–1281, https://doi.org/10.1002/pola.24551.

[13] C. Zhu, L. Yang, C. Chen, G. Zeng, Metal-free recycling of waste polyethylene terephthalate mediated by TBD protic ionic salts: the crucial role of anionic ligands †, (2023) 27936–27941. Doi: 10.1039/d3cp03590e.

[14] R. Nisticò, Polyethylene terephthalate (PET) in the packaging industry, Polym. Test. 90 (2020), https://doi.org/10.1016/j.polymertesting.2020.106707.

[15] F. Pardal, G. Tersac, Comparative reactivity of glycols in PET glycolysis, Polym. Degrad. Stab. 91 (2006) 2567–2578, https://doi.org/10.1016/j.polymdegradstab.2006.05.016.

[16] F. Pardal, G. Tersac, Kinetics of poly(ethylene terephthalate) glycolysis by diethylene glycol. I. Evolution of liquid and solid phases, Polym. Degrad. Stab. 91 (2006) 2840–2847, https://doi.org/10.1016/j.polymdegradstab.2006.09.009.

[17] Z. Fehér, J. Kiss, P. Kisszékelyi, J. Molnár, P. Huszthy, L. Kárpáti, J. Kupai, Optimisation of PET glycolysis by applying recyclable heterogeneous organocatalysts, Green Chem. 24 (2022) 8447–8459, https://doi.org/10.1039/d2gc02860c.

[18] R. López-Fonseca, I. Duque-Ingunza, B. de Rivas, L. Flores-Giraldo, J.I. Gutiérrez-Ortiz, Kinetics of catalytic glycolysis of PET wastes with sodium carbonate, Chem. Eng. J. 168 (2011) 312–320, https://doi.org/10.1016/j.cej.2011.01.031.

[19] M.E. Viana, A. Riul, G.M. Carvalho, A.F. Rubira, E.C. Muniz, Chemical recycling of PET by catalyzed glycolysis: Kinetics of the heterogeneous reaction, Chem. Eng. J. 173 (2011) 210–219, https://doi.org/10.1016/j.cej.2011.07.031.

[20] B. Liu, X. Lu, Z. Ju, P. Sun, J. Xin, X. Yao, Q. Zhou, S. Zhang, Ultrafast homogeneous glycolysis of waste polyethylene terephthalate via a dissolution-degradation strategy, Ind. Eng. Chem. Res. 57 (2018) 16239–16245, https://doi.org/10.1021/acs.iecr.8b03854.

[21] N.H. Le, T.T. Van Ngoc, B. Shong, J. Cho, Low-Temperature Glycolysis of Polyethylene Terephthalate, ACS Sustain. Chem. Eng. 10 (2022) 17261–17273, https://doi.org/10.1021/acssuschemeng.2c05570.

[22] M. Crippa, B. de Wilde, R. Koopmans, J. Leyssens, J. Muncke, A. Ritschkoff, K. van Doorsselaer, C. Velis, M. Wagner, A circular economy for plastics-Insights from research and innovation to inform policy and funding decisions, Brussels (2019), https://doi.org/10.2777/269031.

[23] H. Essaddam, Polyethylene Terephthalate depolymerization, US 9550713 B1, 2017.

[24] T. Haga, Anomalous Swelling of Poly(ethylene Terephthalate) Fiber in Organic Solvents, Polymer Letters. 20 (1982) 629–634, https://doi.org/10.1002/pol.1982.130201204.

[25] S. Zhang, W. Xu, R. Du, W. An, X. Liu, S. Xu, Y.Z. Wang, Selective depolymerization of PET to monomers from its waste blends and composites at ambient temperature, Chem. Eng. J. 470 (2023), https://doi.org/10.1016/j.cej.2023.144032.

[26] C.M. Alder, J.D. Hayler, R.K. Henderson, A.M. Redman, L. Shukla, L.E. Shuster, H. F. Sneddon, Updating and further expanding GSK's solvent sustainability guide, Green Chem. 18 (2016) 3879–3890, https://doi.org/10.1039/c6gc00611f.

[27] J. Huang, D. Yan, Q. Zhu, X. Cheng, J. Tang, X. Lu, J. Xin, Depolymerization of polyethylene terephthalate with glycol under comparatively mild conditions, Polym. Degrad. Stab. 208 (2023), https://doi.org/10.1016/j.polymdegradstab.2022.110245.

[28] S. Farah, K.R. Kunduru, A. Basu, A.J. Domb, Molecular Weight Determination of Polyethylene Terephthalate, Poly(Ethylene Terephthalate) Based Blends, Composites and Nanocomposites. (2015) 143–165. https://doi.org/10.1016/B978-0-323-31306-3.00008-7.

[29] I. Flores, J. Demarteau, A.J. Müller, A. Etxeberria, L. Irusta, F. Bergman, C. Koning, H. Sardon, Screening of different organocatalysts for the sustainable synthesis of PET, Eur. Polym. J. 104 (2018) 170–176, https://doi.org/10.1016/j.eurpolymj.2018.04.040.

[30] I. Flores, A. Etxeberria, L. Irusta, I. Calafel, J.F. Vega, J. Martínez-Salazar, H. Sardon, A.J. Müller, PET- ran-PLA Partially Degradable Random Copolymers Prepared by Organocatalysis: Effect of Poly(l -lactic acid) Incorporation on Crystallization and Morphology, ACS Sustain. Chem. Eng. 7 (2019) 8647–8659, https://doi.org/10.1021/acssuschemeng.9b00443.

[31] I. Flores, A. Basterretxea, A. Etxeberria, A. González, C. Ocando, J.F. Vega, J. Martínez-Salazar, H. Sardon, A.J. Müller, Organocatalyzed Polymerization of PET- mb-poly(oxyhexane) Copolymers and Their Self-Assembly into Double Crystalline Superstructures, Macromolecules 52 (2019) 6834–6848, https://doi.org/10.1021/acs.macromol.9b01110.

[32] R. Ibbett, NMR Spectroscopy of Polymers, 1st ed., Springer Science+Business Media Dordrecht, Glasgow, 1993. Doi: 10.1007/978-94-011-2150-7.

[33] K. Phan, E. Van Den Broeck, K. Raes, K. De Clerck, V. Van Speybroeck, S. De Meester, A comparative theoretical study on the solvent dependency of anthocyanin extraction profiles, J. Mol. Liq. 351 (2022), https://doi.org/10.1016/j.molliq.2022.118606.

[34] C.M. Hansen, Hansen Solubility Parameters A User's Handbook Second Edition, 2nd ed., CRC Press, Boca Raton, 2007.

[35] K. Phan, S. Ügdüler, L. Harinck, R. Denolf, M. Roosen, G. O'Rourke, D. De Vos, V. Van Speybroeck, K. De Clerck, S. De Meester, Analysing the potential of the selective dissolution of elastane from mixed fiber textile waste, Resour. Conserv. Recycl. 191 (2023), https://doi.org/10.1016/j.resconrec.2023.106903.

[36] T. Haga, Case II Swelling of Poly(ethylene Terephthalate) in Organic Solvents, J. Appl. Polym. Sci. 26 (1981) 2649–2655.

[37] W. Ingamells, A. Yabani, The Swelling and Plasticization of Poly(ethylene terephthalate) during Carrier Dyeing, J. Soc. Dye. Colour. 93 (1977) 417–423.

[38] N. Aranburu, J.I. Eguiazabal, Compatible blends of polypropylene with an amorphous polyamide, J. Appl. Polym. Sci. 127 (2013) 5007–5013, https://doi.org/10.1002/app.38090.

[39] Hitachi, Tabletop Microscope TM3030Plus, (2014).

[40] F.K. Metze, S. Sant, Z. Meng, H.A. Klok, K. Kaur, Swelling-Activated, Soft Mechanochemistry in Polymer Materials, Langmuir 39 (2023) 3546–3557, https://doi.org/10.1021/acs.langmuir.2c02801.

[41] P. Majgaonkar, R. Hanich, F. Malz, R. Brüll, Chemical Recycling of Post-Consumer PLA Waste for Sustainable Production of Ethyl Lactate, Chem. Eng. J. 423 (2021), https://doi.org/10.1016/j.cej.2021.129952.

[42] A. Sangalang, L. Bartolome, D.H. Kim, Generalized kinetic analysis of heterogeneous PET glycolysis: Nucleation-controlled depolymerization, Polym. Degrad. Stab. 115 (2015) 45–53, https://doi.org/10.1016/j.polymdegradstab.2015.02.012.

[43] S. Javed, J. Fisse, D. Vogt, Kinetic Investigation for Chemical Depolymerization of Post-Consumer PET Waste Using Sodium Ethoxide, Ind. Eng. Chem. Res. (2022), https://doi.org/10.1021/acs.iecr.2c04308.

[44] J.W. Chen, L.W. Chen, W.H. Cheng, Kinetics of glycolysis of polyethylene terephthalate with zinc catalyst, Polym. Int. 48 (1999) 885–888, https://doi.org/10.1002/(sici)1097-0126(199909)48:9<885::aid-pi216>3.0.co;2-t.

[45] J.R. Campanelli, M.R. Kamal, D.G. Cooper, Kinetics of glycolysis of Poly(Ethylene Terephthalate) Melts, J. Appl. Polym. Sci. 54 (1994) 1731–1740, https://doi.org/10.1002/app.1994.070541115.

[46] K. Ravindranath, R.A. Mashelkar, Polyethylene terephthalate- I. Chemistry, Thermodynamics and Transport Properties, Chem. Eng. Sci. 41 (1984) 2197–2214, https://doi.org/10.1016/0009-2509(86)85070-9.

[47] D. Lei, X.L. Sun, S. Hu, H. Cheng, Q. Chen, Q. Qian, Q. Xiao, C. Cao, L. Xiao, B. Huang, Rapid Glycolysis of Waste Polyethylene Terephthalate Fibers via a Stepwise Feeding Process, Ind. Eng. Chem. Res. 61 (2022) 4794–4802, https://doi.org/10.1021/acs.iecr.1c05022.

[48] O. Levenspiel, Fluid-Particle Reactions: Kinetics, in: Chemical Reaction Engineering , 3rd ed., John Wiley & Sons, 1999: pp. 668.

[49] H.S. Fogler, Leyes de velocidad y estequiometría, in: Bernard M. Goodwin (Ed.), Elements of Chemical Reaction Engineering , 3rd ed., 1999: pp. 65–69.

[50] G. O'Rourke, M. Houbrechts, M. Nees, M. Roosen, S. De Meester, D. De Vos, Delamination of polyamide/polyolefin multilayer films by selective glycolysis of polyurethane adhesive, Green Chem. 24 (2022) 6867–6878, https://doi.org/10.1039/d2gc01531e.

[51] S. Ügdüler, K.M. Van Geem, R. Denolf, M. Roosen, N. Mys, K. Ragaert, S. De Meester, Towards closed-loop recycling of multilayer and coloured PET plastic waste by alkaline hydrolysis, Green Chem. 22 (2020) 5376–5394, https://doi.org/10.1039/d0gc00894j.
[52] J. Huang, D. Yan, H. Dong, F. Li, X. Lu, J. Xin, Removal of trace amount impurities in glycolytic monomer of polyethylene terephthalate by recrystallization, J. Environ. Chem. Eng. 9 (2021) 106277, https://doi.org/10.1016/j.jece.2021.106277.
[53] H. Yao, D. Yan, X. Lu, Q. Zhou, Y. Bao, J. Xu, Solubility determination and thermodynamic modeling of bis-2-hydroxyethyl terephthalate (BHET) in different solvents, Chin. J. Chem. Eng. 45 (2022) 294–300, https://doi.org/10.1016/j.cjche.2021.03.024.
[54] K.K. Ghosh, M.L. Satnami, D. Sinha, J. Vaidya, Solvent effects on the nucleophilic substitution reactions of p-nitrophenyl acetate with hydroxamate ions, J. Mol. Liq. 116 (2005) 55–60, https://doi.org/10.1016/j.molliq.2004.06.003.
[55] D. Prat, A. Wells, J. Hayler, H. Sneddon, C.R. McElroy, S. Abou-Shehada, P.J. Dunn, CHEM21 selection guide of classical- and less classical-solvents, Green Chem. 18 (2015) 288–296, https://doi.org/10.1039/c5gc01008j.
[56] N. Jomtib, C. Prommuak, M. Goto, M. Sasaki, A. Shotipruk, Effect of co-solvents on transesterification of refined palm oil in supercritical methanol, Eng. J. 15 (2011) 49–58, https://doi.org/10.4186/ej.2011.15.3.49.
[57] M. Mohan, J.D. Keasling, B.A. Simmons, S. Singh, In silico COSMO-RS predictive screening of ionic liquids for the dissolution of plastic, Green Chem. 24 (2022) 4140–4152, https://doi.org/10.1039/d1gc03464b.
[58] S. Imdad, R.K. Dohare, Preparation of ultrafiltration membrane from discarded polyethylene terephthalate bottles, Environ. Sci. Pollut. Res. (2022), https://doi.org/10.1007/s11356-022-23068-8.
[59] Chanda, Manas, Roy, Salil K, Industrial Polymers, Specialty Polymers, and Their Applications, CRC Press, 2009.
[60] M. Stamm, B. Carlowitz, Ullmann's Polymers and Plastics: Products and Processes, in: Ullmann's Polymers and Plastics, 2016: pp. 471–526.
[61] F.K. Metze, S. Sant, Z. Meng, H.A. Klok, K. Kaur, Swelling-Activated, Soft Mechanochemistry in Polymer Materials, Langmuir (2022), https://doi.org/10.1021/acs.langmuir.2c02801.
[62] A.B. Desai, G.L. Wilkes, Solvent-induced crystallization of Polyethylene terephthalate, J. Polym. Sci., Polym. Symp. 46 (1974) 291–319, https://doi.org/10.1002/polc.5070460123.
[63] E. Afonso, A. Martínez-Gómez, A. Huerta, P. Tiemblo, N. García, Facile Preparation of Hydrophobic PET Surfaces by Solvent Induced Crystallization, Coatings 12 (2022), https://doi.org/10.3390/coatings12020137.
[64] H. Ouyang, W.H. Lee, W. Ouyang, S.T. Shiue, T.M. Wu, Solvent-induced crystallization in poly(ethylene terephthalate) during mass transport: Mechanism and boundary condition, Macromolecules 37 (2004) 7719–7723, https://doi.org/10.1021/ma0400416.
[65] B.A. Miller-Chou, J.L. Koenig, A review of polymer dissolution, Progress in Polymer Science (Oxford). 28 (2003) 1223–1270. Doi: 10.1016/S0079-6700(03)00045-5.
[66] R.B. Bird, W.E. Stewart, E.N. Lightfoot, Chapter 17 Diffusivity and the mechanisms of mass transport, in: Transport Phenomena, John Wiley & Sons, Inc., 2002: pp. 513–539.
[67] P.T. Anastas, D.G. Hammond, Chapter 4 - Case Studies — Green Chemistry in Practice, in: Inherent Safety At Chemical Sites: Reducing Vulnerability to Accidents and Terrorism Through Green Chemistry, Elsevier Inc., 2016: pp. 23–118. Doi: 10.1016/B978-0-12-804190-1.00004-5.
[68] K. Bose, K.K. Kundu, Ionization of ethylene glycol in isodielectric acetonitrile + ethylene glycol mixtures at 25 °C, Can. J. Chem. 57 (1979) 2470–2475, https://doi.org/10.1139/v79-393.
[69] J.S. Papanu, D.W. Hess, D.S. Soane, A.T. Bell, Dissolution of Thin Poly(methyl methacrylate) Films in Ketones, Binary Ketone/Alcohol Mixtures, and Hydroxy Ketones, n.d.
[70] A. Gigliuzza, Solvent Swollen Polymer, in: L. Giorno, E. Drioli (Eds.), Encyclopedia of Membranes, Springer Berlin Heidelberg, 2016: pp. 1801–1803. Doi: 10.1007/978-3-662-44324-8.
[71] M. Zaborowska, K. Bernat, The development of recycling methods for bio-based materials – A challenge in the implementation of a circular economy: A review, Waste Manag. Res. 41 (2023) 68–80, https://doi.org/10.1177/0734242X221105432.
[72] Z. Chen, M.J. Jenkins, J.N. Hay, Annealing of poly (ethylene terephthalate), Eur. Polym. J. 50 (2014) 235–242, https://doi.org/10.1016/j.eurpolymj.2013.11.004.
[73] R. Ratti, Industrial applications of green chemistry: Status, Challenges and Prospects, SN Appl Sci. 2 (2020), https://doi.org/10.1007/s42452-020-2019-6.
[74] D. Civancik-Uslu, T.T. Nhu, B. Van Gorp, U. Kresovic, M. Larrain, P. Billen, K. Ragaert, S. De Meester, J. Dewulf, S. Huysveld, Moving from linear to circular household plastic packaging in Belgium: Prospective life cycle assessment of mechanical and thermochemical recycling, Resour. Conserv. Recycl. 171 (2021), https://doi.org/10.1016/j.resconrec.2021.105633.
[75] European Comission, A European Green Deal, (2020). https://commission.europa.eu/strategy-and-policy/priorities-2019-2024/european-green-deal/repowereu-.